TECHNISCHE
UNIVERSITÄT
WIEN

**Master Thesis**


# LIGAND DESIGN FOR

# ASYMMETRIC TRANSFER HYDROGENATIONS

# IN AQUEOUS MEDIUM


Ausgeführt am

Institut für Angewandte Synthesechemie


Unter der Leitung von

Ass.Prof. Dipl.-Ing. Dr.techn. Katharina Schröder


eingereicht an der Technischen Universität Wien

am 09.03.2017

von


BSc. Jacqueline Bitai

Matrikelnummer: 1025799

Fellnergasse 3/7/8

1220 Wien

# Table of Contents

# Abstract

The present thesis focuses on the synthesis of new chiral ionic ligands designed to fulfill the requirements for the application in asymmetric transfer hydrogenations.

Based on a chiral amino alcohol and a chiral diamine structural motive, highly coordinating chiral ionic ligands with bidentate structural motive were obtained. By introducing an ionic head group, the solubility of the designed ligands could be adapted via the choice of anion. Moreover, different substitution patterns for diamine based chiral ionic ligands were exploited.

The newly designed ligands were successfully applied in transition metal catalyzed asymmetric transfer hydrogenation in aqueous medium. By taking advantage of the tunable properties of the designed ligands, their positive effect on asymmetric transfer hydrogenation could be demonstrated.

# Kurzfassung

Die aktuelle Arbeit beschäftigt sich mit der Synthese neuer chiraler Liganden, welche speziell für die Anwendung in der asymmetrischen Transferhydrierung entwickelt wurden.

Basierend auf der Struktur chiraler Aminoalkohole und chiraler Diamine konnten stark koordinierende, chirale ionische Liganden erhalten werden. Durch die Einführung einer ionischen Gruppe konnte die Löslichkeit der entwickelten Liganden durch die Wahl des Anions modifiziert werden. Außerdem wurden verschiedene Substitutionsmuster im Fall der Diamin-basierten Liganden getestet.

Die neu entwickelten Liganden konnten erfolgreich in der Übergangsmetall katalysierten asymmetrischen Transferhydrierung in wässrigem Medium eingesetzt werden. Unter Ausnützung der veränderlichen Eigenschaften der Liganden konnte deren positiver Effekt auf die asymmetrische Transferhydrierung demonstriert werden.

# I    Introduction

Catalytic transformations are becoming increasingly important, not only for industrial processes, but also in laboratory applications. Especially under the aspect of environmental concerns and sustainability issues, catalysis plays a major role. Using catalytic rather than stoichiometric reagents is a key aspect of the 12 principles of green chemistry,[1] but also contributes to other points, such as atom efficiency and waste prevention. Since the discovery of the first catalytic reaction around 1900 by Sabatier, who found that nickel is an active catalyst in hydrogenation reactions,[2] catalysis has become an important strategy for industrial processes. However, in organic chemistry catalytic protocols have been less common, with the preference lying on stoichiometric reagents for which the reactions are well understood and reliable. This difference in the preferred methods can be reflected in the waste production in different industry segments (Table 1). Whilst oil refining and the production of bulk chemicals relies on catalytic transformations, the synthesis of fine chemicals and pharmaceuticals is rather the domain of organic chemists, who often prefer stoichiometric reagents.

*Table 1: Production waste volume in different chemical industry segments.*[3]

| Industry segment | Product tonnage | kg waste[a] / kg product |
|---|---|---|
| Oil refining | $10^6 - 10^8$ | $< 0.1$ |
| Bulk chemicals | $10^4 - 10^6$ | $< 1 - 5$ |
| Fine chemicals | $10^2 - 10^4$ | $5 - 50$ |
| Pharmaceuticals | $10 - 10^3$ | 25 - 100 |

*[a] defined as all materials produced except the desired product*
*(including all inorganic salts, solvent losses, etc.).*

Amongst the many transformations encountered in chemistry, reductions of unsaturated compounds to their saturated analogues occupy a central place. Within those, carbonyl compounds are key substrates and the reduction to the corresponding alcohols is a reaction widely used. Therefore, a variety of different reduction protocols have been developed. In general, they can be divided into stochiometric and catalytic procedures, as depicted in Figure 1. For small-scale applications, carbonyl reductions are preferably performed using stoichiometric reagents, such as sodium borohydride or lithium aluminum hydride. In industry, on the other hand, catalytic reduction procedures are very well established. Within those hydrogenations using hydrogen gas as the reducing agent constitute to a great part of the chemical industry. They are used in the petrochemical industry for oil refining, in food industry to produce fats, or in the production of bulk and fine chemicals. Furthermore, a subdivision within the catalytic procedures into heterogeneous and homogeneous methods is possible.
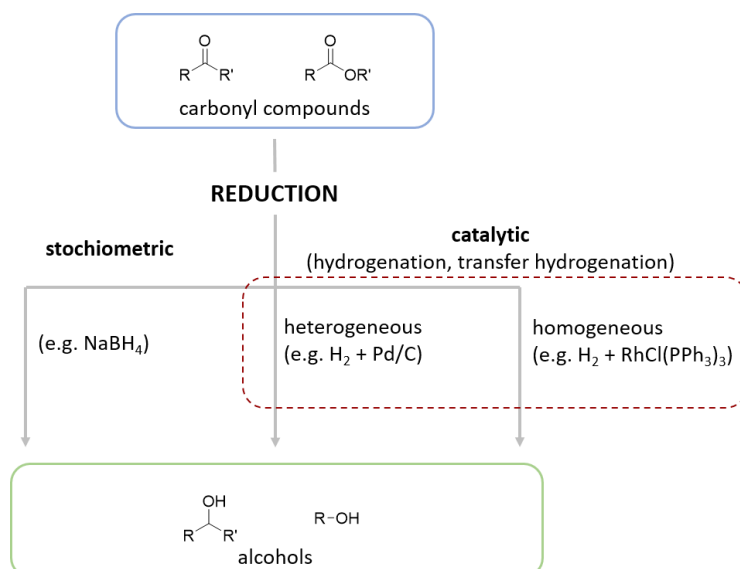
*Figure 1. Reduction methods for carbonyl compounds*

For these industrial processes a heterogenous metal catalyst such as nickel or palladium on a solid support is most commonly applied in combination with hydrogen under high temperatures and pressures to convert carbonyl compounds such as aldehydes or ketones into the corresponding alcohols.[4] Hydrogenations relying on heterogeneous catalysis and hydrogen as reducing agent offer some advantages:

(1) fast and easy product separation from the catalyst, for example by simple filtration

(2) broad substrate scope – hydrogenation of many functional groups possible

(3) build on long-time experience – well established process technology, straightforward scale up

(4) easy implementation of a continuous process

Nonetheless, some problematic aspects have to be considered, especially concerning hydrogenations using hydrogen gas. The use of molecular hydrogen as the reducing agent inherits some major safety risks. Hydrogen gas is easily inflammable and due to its high diffusibility rather hard to control and difficult to store. Furthermore, the reactions have to be conducted under pressurized conditions, which not only poses operational risks, but also calls for specialized equipment. These are major drawbacks, especially for small scale productions and laboratory applications.

Consequently, transfer hydrogenations have emerged as alternative catalytic procedure for the reduction of a number of functional groups. In this strategy, small organic molecules such as alcohols or formic acid are used as hydrogen source instead of molecular hydrogen, employing either a heterogeneous or homogeneous catalyst. Since the setup for transfer hydrogenations is straightforward and does not require any specialized pressure equipment, it now finds its way not only into laboratory applications, but also into industry as a complementing technique to common hydrogenations.[5,6]

In fact, some transfer hydrogenations are already implemented in the production of optically active agricultural or pharmaceutical chemicals.[7] For example, an intermediate in the synthesis of the herbicide (*S*)-MA20565 is produced using the Ru catalyzed asymmetric transfer hydrogenation with 2-propanol as hydrogen donor on a 100 kg scale (Scheme 1).
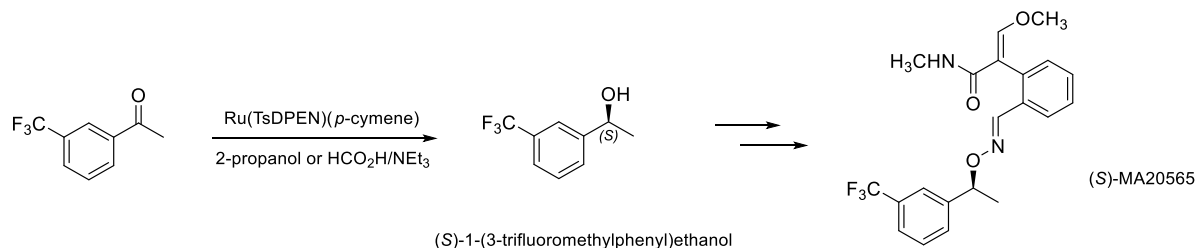


*Scheme 1. Large scale transfer hydrogenation process to produce an agrochemical*

Enantioselective transformation such as the example presented above are usually performed in a homogeneous fashion, since common heterogeneous catalysts are not able to perform well in these reactions. Therefore, homogeneous reaction protocols for the reduction of carbonyl compounds via hydrogenations and transfer hydrogenations are of great interest. Since the development of the homogeneous rhodium tris(triphenylphosphine) catalyst RhCl(PPh$_3$)$_3$ by Wilkinson and co-workers in 1965 for hydrogenations,[8] homogeneous catalysis has become widely applied. The success of the Wilkinson catalyst further prompted the development of homogeneous enantioselective transformations, as chiral ligands could be included in a homogeneous, well defined catalyst. In general, a homogeneous process features a catalyst dissolved in the reaction media alongside with the substrates and products. This allows for mild reaction conditions, high activity and selectivity as well as for an efficient heat transfer. Transfer hydrogenations in particular seem to be ideally suited for a homogeneous setup, as the organic molecules used as hydrogen donors can be dissolved in the reaction mixture. Hence, not only the use of hydrogen gas can be avoided, but also mixing issues of the hydrogen gas in the liquid reaction medium can be circumvented.

However, besides the attractive features that a homogenous transfer hydrogenation set-up offers, it still suffers from some drawbacks:

   (1)  cumbersome recovery of the expensive catalysts

   (2)  limited availability of catalysts and ligands compared to conventional hydrogenations

   (3)   difficult scale up and implementation of a continuous process

To overcome these barriers, research focused intensively on transfer hydrogenations over the last decades, especially regarding asymmetric transformations. The selectivity in terms of chemo-, stereo- and regioselectivity can be different from the ones obtainable by asymmetric hydrogenations, since different mechanisms are operating. Hence, asymmetric transfer hydrogenations may complement asymmetric hydrogenations.[9]

## I.1    Transfer Hydrogenation

A hydrogen transfer reaction is defined as "the reduction of multiple bonds with the aid of a hydrogen donor in the presence of a catalyst".[10] In this case the donor molecule must be different from hydrogen gas and is usually a small organic molecule such as isopropanol or formic acid. By avoiding hydrogen gas, the process becomes inherently safer and simpler to operate, since no specialized pressure reactors are needed. Furthermore, the employed hydrogen donors are readily available, cheap and easy to handle.

The first reported transfer hydrogenation dates back to 1925.[11–13] In this reaction aluminum isopropoxide was used to reduce carbonyl compounds to the corresponding alcohols by using isopropanol as the hydrogen donor (see Scheme 2) Today this transformation is known as the Meerwein-Ponndorf-Verley (MPV) reduction.
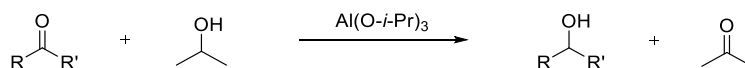


*Scheme 2. Meerwein-Ponndorf-Verley reduction*

In the 1960s and 70s the first publications on transition metal catalyzed transfer hydrogenations based on Ir- or Ru-complexes appeared in the literature.[14,15] Ever since, great improvement has been made in the field of transfer hydrogenations: the variety and efficiency of catalysts has been improved and the substrate scope expanded. Therefore, transfer hydrogenation reactions are applicable to the reduction of C=O and C=N double bonds, for example in ketones, aldehydes or imines as well as to chemoselective reductions of carbonyl functionalities in ketoesters or α,β-unsaturated ketones. Moreover, C–C double and triple bonds can also be reduced. In the following paragraphs the underlying principles in transfer hydrogenation reactions will be discussed and different hydrogen donors will be evaluated.

## I.1.1    Mechanism

It is commonly accepted that two substantially different mechanisms are at work in transfer hydrogenations depending on the metal catalyst employed. Therefore, the following two mechanisms have been proposed: (a) direct hydrogen transfer; (b) hydridic route.[10,16]

(a) Direct Hydrogen Transfer

Direct hydrogen transfer proceeds via a concerted pathway in which the hydrogen donor and the hydrogen acceptor coordinate simultaneously to the metal center, forming a six-membered cyclic transition state to enable the hydride transfer (Scheme 3). This mechanism is operating with

non-transition metals such as aluminum or samarium and is similar to the one proposed for the MPV reduction.
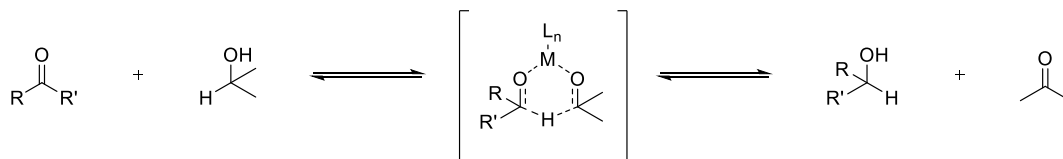


*Scheme 3. Direct hydrogen transfer mechanism*

(b) Hydridic Route

In this case a stepwise mechanism is operating, where a metal hydride is formed as active intermediate (Scheme 4). In the first step the hydrogen donor interacts with the metal center. Upon dissociation, the intermediate metal hydride is being formed, leading consequently to the oxidation of the hydrogen donor. In the second step the hydrogen acceptor coordinates to the metal center. Thereby the hydride transfer to the organic molecule takes place, resulting in the reduced compound. This mechanism is operating for transition metal based catalysts, e.g. Ru, Rh or Ir species.
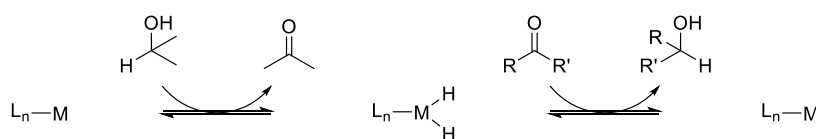


*Scheme 4. Hydridic route*

## I.1.2    Hydrogen Donors

Hydrogen donors most frequently used in the literature are secondary alcohols and formic acid. Amongst secondary alcohols, isopropanol is most prominent. It is inexpensive, readily available, easy to handle, nontoxic and considered as environmentally friendly. In addition, it is able to dissolve many organic compounds. When isopropanol is used as the hydrogen donor, an additional base is typically required to convert the catalyst into its active form. For this purpose, inorganic salts such as sodium or potassium carbonates or hydroxides are most commonly employed. In the course of the reaction isopropanol is oxidized to acetone. However, acetone can participate in the catalytic cycle as well, thereby posing the problem of reaction reversibility. Especially with ketones the reaction equilibrium lies preferentially on the side of the corresponding alcohol. Consequently, isopropanol is typically also used as the solvent of the reaction, thereby shifting the reaction equilibrium towards the desired product. Another possibility is to remove the formed acetone by distillation during the reaction. However, this often complicates the reaction setup. The reversibility of the reaction is the major drawback when using isopropanol. This becomes especially pronounced for asymmetric reactions, as higher conversions lead to the erosion of the enantiomeric purity of the product.[17]

Another commonly used hydrogen donor is formic acid employed as an azeotropic 5:2 mixture with triethylamine. In comparison to isopropanol the dehydrogenation of formic acid is an irreversible process, since the formed product $CO_2$ will evolve from the reaction mixture. Thus, high conversions can be obtained without the drawback of reversibility or, in case of enantioselective reactions, racemization. However, the rather low pH encountered in this system leads to the decomposition of several catalyst complexes, while others are inhibited due to formic acid preventing the formation of the active catalyst.[17]

Besides formic acid, its salts are also encountered as hydrogen donors. Especially since 2000, sodium formate as hydrogen donor in combination with water as the solvent has emerged as useful and green alternative to the traditional donor/solvent systems. Since sodium formate is oxidized to $CO_2$ during the catalytic cycle, the reaction is also irreversible. In contrast to formic acid, the sodium salt exhibits basic properties, thereby circumventing the pH related problems implied by the former. The implications of water on the reaction will be dealt with in detail in I.4.

## I.2 Asymmetric Reductions

Optically active compounds play a central role in all biological processes. Amongst enantiopure small molecules, chiral alcohols are particularly important building blocks in the synthesis of pharmaceuticals, flavors or agricultural chemicals.[18] In general, there are four possibilities for obtaining chiral secondary alcohols from the corresponding ketones via catalytic transformations as shown in Figure 2.
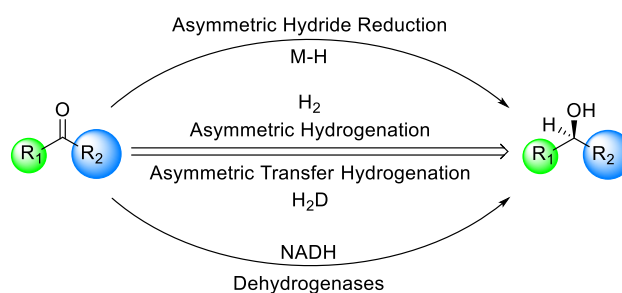


*Figure 2. Asymmetric reduction possibilities; adapted from X. Wu and J. Xiao[18]*

In biological systems, enzymes are the catalysts for various transformations and usually the products are obtained in very high enantioselectivity or even as sole enantiomer. For reductions, enzymes such as dehydrogenases are at work, using the cofactor NAD(P)H as hydrogen donor. However, such enzymatic reactions are more frequently used in laboratory applications, as scale-up still poses a number of issues.

More common are artificial and metal based reduction strategies, including asymmetric hydride reduction, asymmetric hydrogenation and asymmetric transfer hydrogenation. Within the area of catalytic asymmetric hydride reduction, the most applicable catalyst is the Corey-Bakshi-Shibata catalyst based on an oxazaborolidine structure (Figure 3, left).[19] For the reaction stoichiometric amounts of achiral borane are needed, which hinder this transformation from being applicable to a wide range of substrates, since many functional groups are not compatible with borane. Moreover, rather high catalyst loadings up to 10 mol% are usually required. Alternatively, the stochiometric reagent BINAL-H, an enantioselective version of the common $LiAlH_4$ reagent with the chiral $C_2$-symmetric ligand BINOL, may reduce ketones to secondary alcohols with high selectivities (Figure 3, right).[20]



CBS catalyst                    active catalyst                    BINAL-H
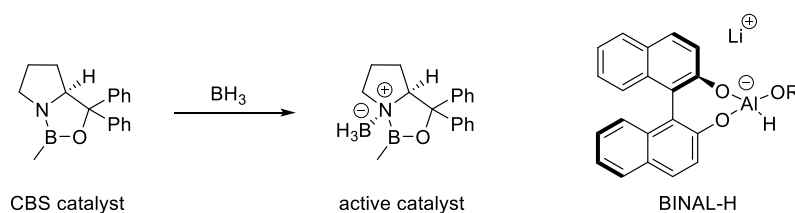
*Figure 3. left: Corey-Bakshi-Shibata (CBS) catalyst; right: BINAL-H*

Asymmetric hydrogenation reactions have been widely studied and are nowadays a very useful and versatile tool for the reduction of many unsaturated molecules. Especially since the development of Noyori's Ru based catalysts for the reduction of carbonyl compounds, which features a chiral diphosphine and a chiral diamine ligand,[21,22] as exemplified in Figure 4, asymmetric hydrogenations have become a key
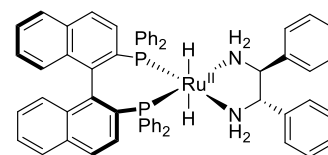


*Figure 4. Example of Ru based Noyori hydrogenation catalyst with BINAP and dpen as chiral ligands*

methodology for the asymmetric reduction of ketones and imines. However, the same risks still hold true which were mentioned earlier, such as the need to work under pressurized conditions with an easily inflammable gas. Moreover, especially in homogeneous systems which are used for asymmetric transformations, the solubility of hydrogen in the corresponding solvent and subsequent mass transport within can be a rate limiting factor.

As a consequence, asymmetric transfer hydrogenation (ATH) is a very promising alternative, which will be discussed in detail in the following sections.

## I.3 Asymmetric Transfer Hydrogenation

Since 1980, when first reports on asymmetric transfer hydrogenation emerged, substantial progress has been made on catalyst and ligand design.[23] Owing to its operational simplicity and adaptability by varying the employed hydrogen source, solvent, transition metal and chiral ligand, ATH has emerged as



$R_n = H$
Me
$1\text{-}CH_3\text{-}4\text{-}CH(CH_3)_2$
$1,3,5\text{-}(CH_3)_3$
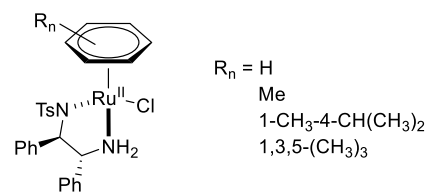
*Figure 5. Noyori-Ikariya catalyst*

a versatile and powerful method for the reduction of ketones. With the discovery of the Noyori-Ikariya catalyst (Figure 5) in 1995,[24] ATH has become a standard approach for asymmetric reductions, alongside with asymmetric hydrogenations. Catalysts used today are most commonly based on ruthenium, although efficient catalysts based on iridium, rhodium and most recently on base metals such as iron have been described as well.[17] A great part of research has been focused on efficient ligand design, aiming at enhancing catalyst activity, stereoselectivity and stability. In the following section a brief assessment of known ligands and their performance will be given.

### I.3.1 Ligands

The ligands used in ATH feature a variety of donor atoms such as nitrogen, oxygen, phosphorus or even sulfur and all possible combinations. Most commonly, chiral bidentate ligands L* are used in combination with an aromatic spectator ligand, which occupies three adjacent coordination sites on the metal center. The chiral induction from the ligand can be enhanced by the proper choice of spectator ligand, since it will also interact with the substrate, hence influencing the stability of the transition state. In the case of Rh or Ir metal centers, cyclopentadienyl based spectator ligands are most commonly applied.[17] For Ru based catalysts benzene derivatives are the usual choice as spectator ligands, whereby the following order of reactivity could be observed: benzene > *p*-cymene ≈ mesitylene > hexamethylbenzene.[5]



$R_n = H_6$: benzene
$Me_6$: hexamethylbenzene
$1\text{-}CH_3\text{-}4\text{-}CH(CH_3)_2$: *p*-cymene
$1,3,5\text{-}(CH_3)_3$: mesitylene

M = Rh(III), Ir(III)
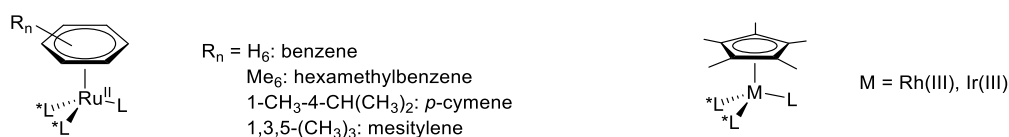
*Figure 6. Common Ru(II), Rh(III) and Ir(III) metal fragments for ATH catalysts*

However, in many well established catalysts one of the sterically more demanding spectator ligands is used, since they give rise to higher enantiomeric excess, although on the expense of catalyst activity. In addition, the employed bidentate ligand has also great influence on catalyst activity and stereoselectivity. Therefore, some prominent chiral ligands and their features will be discussed below.
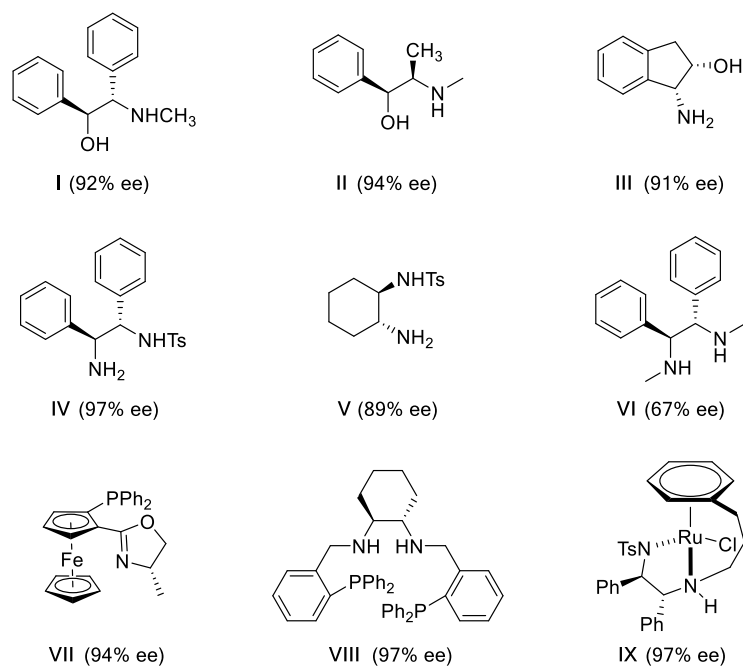
*Figure 7. Common ligands for ATH (ee values are given for the reduction of acetophenone)*

β-Amino alcohol ligands

In the early studies of Noyori, he encountered that simple ethanolamine had the highest acceleration effect on the transfer hydrogenation of acetophenone in isopropanol.[5] This rate enhancement promoted the use of different chiral β-amino alcohols such as 2-amino-1,2-diphenylethanol (**I**), ephedrine (**II**) or 2-amino-1-indanol (**III**).[6] However, β-amino alcohols have been shown to be incompatible with the formic acid-triethylamine mixture as hydrogen donor. This is probably due to the acidic environment inhibiting deprotonation of the hydroxyl group, which is necessary for the formation of the active catalyst.[17]

Diamine ligands

Amongst chiral diamines, monotosylated diamine (**IV**) has shown the second highest acceleration effect after β-amino alcohols. In comparison to β-amino alcohols, diamine ligands are still active in the acidic environment of formic acid-triethylamine as hydrogen donor. This versatility is one of the reasons why this ligand has become the standard choice in ATH and can be used with either ruthenium (termed the Noyori-Ikariya catalyst, see Figure 5),[9] rhodium or iridium. It could be observed that the NH functionality is crucial for the reactivity and enantioselectivity of the catalyst, since the NHCH$_3$ analogue showed much lower reactivity whilst still maintaining comparable enantioselectivity. However, the N(CH$_3$)$_2$ and imine analogues gave very poor reactivity and selectivity.[5]

Ligand (**V**), also bearing a tosyl group and having a rigid cyclohexyl backbone, gave comparable results to (**IV**). It can also be observed that diamines without an electron withdrawing group, such as (**VI**), generally show less reactivity and enantioselectivity.[6]

Other ligands

Besides the two major groups of chiral β-amino alcohol ligands and chiral diamine ligands, many other ligand structures have been explored. For example, the phosphinoxazoline based ligand (**VII**) also showed high reactivity and selectivity.[6]

Besides bidentate ligands, tri- and tetradentate ones are also known. Noyori showed that with the tetradentate ligand (**VIII**) comparable reactivity and stereoselectivity could be obtained.[5] Developments in the recent years yielded some very promising examples of tethered catalysts, in which the chiral ligand is covalently bound to the arene spectator ligand (**IX**).[17]

## I.3.2 Mechanistic understanding

Since the discovery of the very active and selective catalyst RuH[(*R*,*R*)-Tsdpen](η$^6$-*p*-cymene) (Tsdpen = *N*-(*p*-toluenesulfonyl)-1,2-diphenylethylenediamine) by Noyori, Ikariya, Hashiguchi and co-workers, this catalyst has become the number one choice for asymmetric transfer hydrogenation, especially for the reduction of ketones due to its wide applicability while still displaying high reactivity and selectivity. Considerable research efforts in the last two decades have been focusing on this catalyst, aiming to deepen the mechanistic understanding and exploiting the possibilities of ligand modification to find even better catalyst systems. On the following pages the features of this catalyst and the reasons for its unique reactivity and selectivity will be discussed in detail.

In the original work Noyori proposed a catalytic cycle as depicted in Scheme 5.[25] Herein **a** represents the catalyst precursor, which is usually formed in situ by reacting a suitable metal precursor with the desired ligand in the presence of a base. The obtained 18 e$^-$ Ru$^{II}$ complex shows octahedral geometry and is coordinatively saturated. On further treatment with base the true catalyst **b** can be obtained via elimination of HCl. This formal 16 e$^-$ complex shows square planar geometry. Due to the rather basic nitrogen in NR compared to the nitrogen next to the tosyl group, or the oxygen, **b** shows distinct dehydrogenative activity for lower alcohols, such as isopropanol, or formic acid. Therefore, on the interaction with isopropanol a ruthenium hydride **c** is formed as reactive intermediate by the elimination of acetone. This reactive hydride can now reduce a ketone substrate, presumably via the same transition state as operating for the dehydrogenation of isopropanol, whereby the active catalyst **b** is regenerated. The transition states **TS$_{bc}$** and **TS$_{cb}$** display a cyclic, six-membered structure.
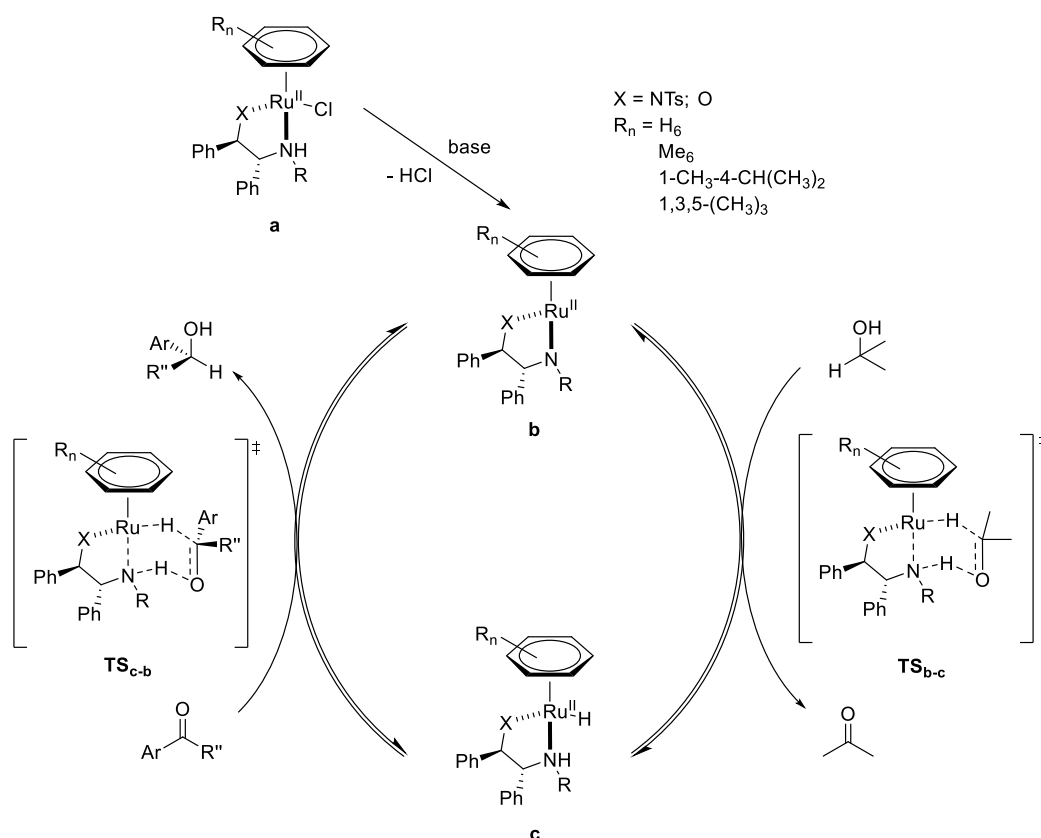
*Scheme 5. Originally proposed catalytic cycle for ATH*

It was proposed that the hydride transfer from ruthenium and the proton transfer from the NH ligand moiety occur in a concerted, pericyclic manner and that the NH linkage furthermore stabilizes the transition state by hydrogen bond formation.[5] Important to note is that the base is only necessary to form the active catalyst **b** from the catalyst precursor **a**. Moreover, the hydrogen transfer between alcohols and carbonyl compounds occurs reversibly during the interconversion of **b** and **c**. Therefore, the desired product formation has to be driven to high conversions by means of shifting the equilibrium, e.g. by using isopropanol in large excess.

Noteworthy is the presumably different mechanism for the formation of the reactive Ru hydride **c** by reaction of the active Ru complex **b** with formic acid as hydrogen donor instead of isopropanol (Scheme 6).[26] In this case a stepwise process is proposed. Formic acid protonates the basic NR nitrogen and the obtained formate ion forms an intermediate ion pair with the protonated Ru complex. This rapidly leads to the formation of the corresponding formato complex, which yields the hydrido Ru complex **c** through decarboxylation. Since this process is again in principle reversible, $CO_2$ should be efficiently removed to avoid the back reaction. However, this is usually not a problem under common reaction conditions, as molecular hydrogen $H_2$, needed for the reverse reaction to formic acid, is not present. Therefore, the process is irreversible.

X = NTs; O    R_n = H_6
                Me_6
                1-CH_3-4-CH(CH_3)_2
                1,3,5-(CH_3)_3
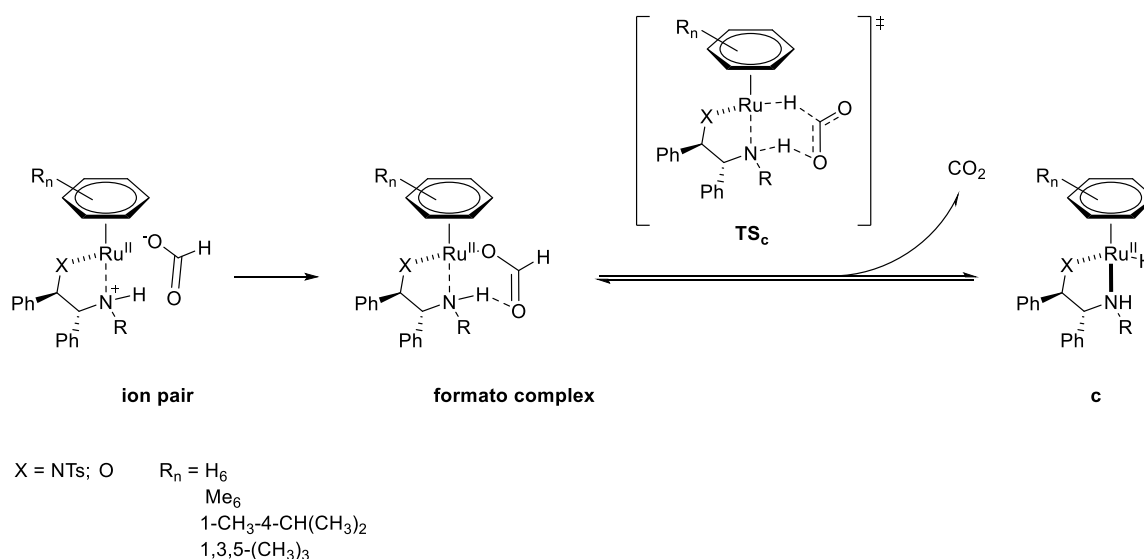
*Scheme 6. Ru hydride regeneration with formic acid as H-donor*

### I.3.2.1    Metal-Ligand Bifunctional Catalysis

The catalytic cycle for the reduction of aromatic ketones shown above represents a novel and non-classical mechanism, termed metal-ligand bifunctional catalysis.[27,28] This implies that the substrate is not directly coordinated to the metal center, as it would be the case for conventional transition metal catalyzed transfer hydrogenation. Instead, it is bound in the outer coordination sphere of the catalyst. The key difference, leading to this new bifunctional mechanism stems from the NH moiety present in the ligand, which is not a mere spectator, but is rather chemically involved in the transformation. This involvement is often termed the "NH effect",[27] and will be discussed in more detail in the following section. This NH unit exhibits sufficiently acidic character to activate the approaching ketone via hydrogen bonding. Through these hydrogen bonding interactions via N−H···O and M−H···C in the outer coordination sphere of the catalyst complex, a six-membered cyclic transition state can be stabilized (see Scheme 5), by which the reduction of the substrate occurs in a concerted transfer of $H^-/H^+$. Thereby, the necessity for a NH functionality in the chiral ligand becomes evident. Moreover, this mechanism is able to explain the uncommon chemoselectivity for the reduction of polarized double bonds such as C=O and C=N over non-polarized C=C double bonds, which need to interact directly with the metal center.

In recent years, new experimental and computational results were found, which seem to contradict the generally accepted mechanism of ATH via a pericyclic transition state. Xiao and coworkers found significant rate acceleration effects when solvents with increasing polarity, such as water, were used.[29] This finding is clearly inconsistent with a pericyclic transition state, in which the charge distribution in the involved complexes and substrates is rather similar. An acceleration in polar solvents would

suggest a transition state that differs considerably in charge distribution from the initial reactants. Moreover, newer computational studies predict a stepwise reduction, where the hydride transfer and the proton transfer would not occur simultaneously.[30,31] Therefore, the transition states leading to both intermediates **b** and **c** must be different, as both species as well as the precatalyst **a** could be isolated and their structure confirmed by X-ray diffraction.[25] The inconsistency between these new findings and the widely accepted concerted mechanism can be explained by a more critical assessment of the earlier studies. The pericyclic transition state was supported by computational studies performed in the gas phase,[27] where no solvent interactions would need to be considered. Reactions in the gas phase proceed preferably without charge separation or distribution, therefore supporting a pericyclic transition state. However, the reactions are not performed in the gas phase, but in a solvent.
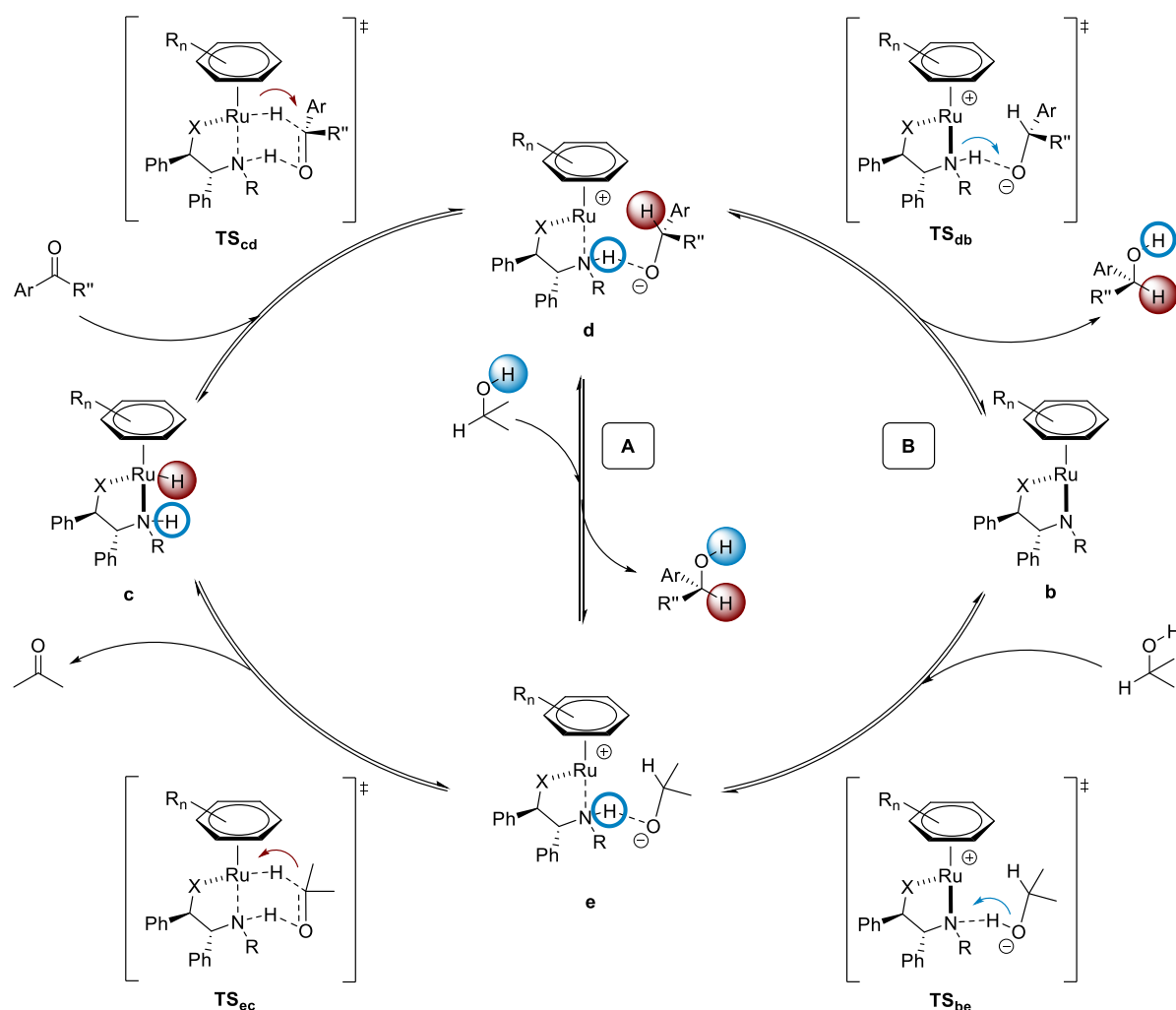


*Scheme 7. Revised catalytic cycle featuring an intermediate ion pair*

A newer and more appropriate quantum chemical calculation has been conducted to further investigate those contradicting experimental results, taking solvent effects into account by using continuum and discrete solvation models.[31] The new calculations revealed that a concerted process

does not exist in solution. They suggest that the ketone is rather reduced in a stepwise manner starting with hydride transfer followed by proton transfer. This consecutive process further leads to the existence of an intimate ion pair, though very likely with a short lifetime, as was already suggested for the regeneration of the Ru hydride **c** by formic acid. The revised catalytic cycle for the asymmetric transfer hydrogenation of acetophenone in isopropanol as supported by the recent computational results is depicted in Scheme 7. As can be seen, hydride transfer from **c** to acetophenone still takes place via a cyclic transition state **TS_cd**. However, only the hydride is delivered to the ketone in this step, leading to the formation of an intimate ion pair **d** of the cationic complex and the anionic alkoxy ion. This ion pair is not only stabilized by coulombic interactions, but also by classical N−H···O hydrogen bonding as well as non-classical C−H···M hydrogen bonding. It has also been found that the hydride transfer is the enantio- and rate determining step.[31] From that point onwards, two pathways are possible for the proton transfer to the alkoxy ion: either via the NH moiety of the ligand (path **B**) or via a solvent molecule (path **A**). The first possibility, proton transfer from the NH moiety of the ligand (path **B**), is in analogy to what was already assumed for the original catalytic cycle (Scheme 5). Through the NH proton transfer, the reduced product is released and the Ru amido complex **b** is formed. To regenerate the Ru hydride complex **c** the same steps will be repeated: coordination of isopropanol to the ligand via hydrogen bonding, formation of an intimate ion pair **e**, followed by hydrogen transfer to the ruthenium metal center. Thereby, acetone is released and complex **c** regenerated. However, the proton can also be delivered by a solvent molecule. In this case the alkoxy ion would abstract the proton from the hydrogen donating isopropanol, forming the neutral product, and the isopropoxide ion forms an intimate ion pair **e** with the cationic ruthenium complex, stabilized by hydrogen bonding with the NH moiety. For this pathway, the ligand would not participate in the catalytic reaction. Moreover, this pathway proceeds without the formation of the intermediate amido complex **b**. Both pathways seem to be operating simultaneously. Depending on the exact reaction conditions, one might be favored over the other. It seems that with increasing solvent polarity, proton transfer from a solvent molecule becomes more probable.[31]

## I.3.2.2    NH Effect

The "NH effect" refers to the necessity of a primary or secondary amine functionality in the chiral ligand, as this feature is crucial for obtaining a highly reactive and selective ATH catalyst. Since the discovery of this effect by Noyori and co-workers,[5] many investigations regarding the processes occurring in an asymmetric transfer hydrogenation have been going on. Although changes to the originally described
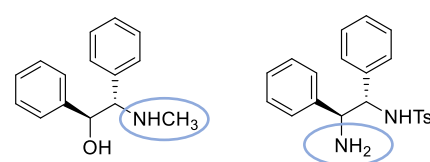
*Figure 8. ATH ligands possessing a primary or secondary amine functionality*

catalytic cycle have been proposed lately, the role of the NH functionality has been undoubted. Its purpose is primarily the coordination of the ketone substrate via hydrogen bonding to activate the ketone for hydride transfer and to stabilize the transition state. Following the revised catalytic cycle (Scheme 7), the NH functionality of the chiral ligand can participate in the bond formation/cleaving processes via proton transfer, but does not necessarily have to. Especially with increasing solvent polarity, the NH functionality remains chemically unmodified throughout the catalytic cycle, as the solvent is the proton source for neutralizing the formed alkoxy ion. In this sense the NH ligand is chemically innocent.

Considering the purpose of the NH functionality, the previously observed order of reactivity $NH_2 > NHR > NR_2$ can be explained.[5] By replacing a hydrogen atom with an alkyl group, the steric demand increases. As a result the accessibility of the hydride atom from the outer sphere becomes more aggravated.[9] In addition, if both hydrogen atoms on the nitrogen are replaced there is no possibility for hydrogen bonding. This explains the virtual inactivity of such disubstituted amine ligands. Another aspect that has to be considered is the acidity of the NH functionality.[32] On one hand, increasing the acidity of the N−H proton will lead to a stronger hydrogen bond to the carbonyl oxygen, lowering the activation barrier for hydride transfer even more, hence enabling a faster reaction. On the other hand, this will lead to a reduced basicity of the amine in the Ru amido complex, resulting in a reduced dehydrogenative activity to regenerate the Ru hydride complex. Therefore, it is important to adjust the acidity/basicity of the NH functionality in a way that neither of the two steps is strongly favored/disfavored.

### I.3.2.3   Effects on Reactivity

Apart from the NH effect or the bulkiness of the aromatic spectator ligand (I.3.1, I.3.2.2) additional factors influencing the reactivity of the catalyst have been identified. In his early work, Noyori observed a dramatic influence of the nitrogen substituent in the chiral diamine ligand on the catalyst reactivity.[5,24] Complexes with a $CF_3SO_2$, $C_6H_5CO$ or $CH_3CO$ substituent on the nitrogen instead of the tosyl group showed far lower reactivity. It has been concluded that the electron withdrawing tosyl group is necessary to increase the acidity of the proton attached to the same nitrogen, thereby facilitating complexation. However, if the electron withdrawing effect of the substituent is too pronounced, the reactivity of the catalyst will nevertheless go down, explaining why $CF_3SO_2$ is a worse substituent than $p$-$CH_3$−$C_6H_4SO_2$. Moreover, it seems that the tosyl group is stabilizing the five-membered chelate ring formed by the diamine ligand and the metal.[27] The influence of the chelate ring conformation, and its resulting stability was also observed by Wills, who found that a matched combination of the two stereogenic centers in the Tsdpen ligand is required for a high reaction rate.[33]

### I.3.2.4    Origin of Enantioselectivity

The enantiodetermining step in an asymmetric transfer hydrogenation is the hydride transfer. Since the NH functionality plays a crucial role in this step by stabilizing the transition state, it can also be assumed that it plays an important part in stereoselection by positioning the substrate in the outer coordination sphere.[9]

Another important part can be attributed to the aromatic spectator ligand. In fact, the C−H···π attractive interaction between the $\eta^6$ ligand and the π-cloud of the approaching aromatic ketone are the main reason for enantioselectivity, since those interactions stabilize the transition state leading to the major enantiomer. This also explains the poor enantioselectivity obtained for dialkyl ketones, since no π-system is available for interactions with the arene ligand. However, it could be observed that with increasing steric demand of those arene ligands, higher ee values can be obtained.[17]

In addition, the tosyl group in the Tsdpen ligand is contributing to the enantioselectivity of the reaction. The interaction of the oxygen lone pairs and the π-cloud of the approaching aromatic ketone leads to a repulsion between those two, thereby destabilizing the less favored diastereomeric transition state. The combination of the attractive C−H···π interaction and the $SO_2$−π repulsion in the case of the Tsdpen ligand leads to a greater energy difference between the diastereomeric transition states, contributing to the excellent ee values obtained. In fact, the presence of the tosyl group is the sole reason why the diamine ligand gives higher enantioselectivities than the otherwise identical β-amino alcohol ligand.[31] Another factor influencing the stereochemical outcome of asymmetric transfer hydrogenations is the conformation of the five-membered chelate ring formed from the ligand and the metal center. The three possible ring conformers are depicted in Figure 9. However, there is more than one stable conformer possible, also depending on the exact position of the substituents and the catalyst diastereomer. Considering this in combination with the other factors mentioned earlier, it is quite difficult to predict the direct influence on the enantioselectivity.[9]



λ-puckered ring          symmetric envelope          δ-puckered ring
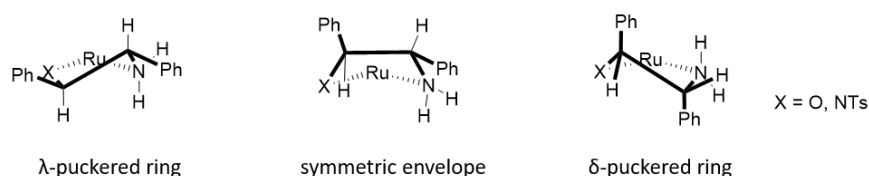
*Figure 9. Possible ring conformers formed by the Ru center and the chiral bidentate ligand*

## I.3.2.5    Substrate Scope

The excellent performance of the Noyori-Ikariya catalyst is the consequence of a compromise between steric and electronic factors of the employed chiral ligand and aromatic spectator ligand combination. This has led to the successful application in the reduction of various substrates. One notable property is the chemoselectivity for carbonyl groups in particular. Therefore, many functional groups are tolerated, such as amino, hydroxyl, chloride, sulfone or ester groups as well as heterocycles.[7] In addition, reductions which are difficult to achieve with hydrogenation catalysts, such as the reduction of tetralone, α-heteroatom substituted aryl ketones and α,β-acetylenic ketones have already been accomplished, again highlighting the great potential of ATH as a complementing method to asymmetric hydrogenation.[18]

In the case of α,β-unsaturated carbonyl compounds, the reduction proceeds preferentially at the carbonyl group, leaving the C=C double bond intact. Nonetheless, careful choice of the appropriate catalyst will be important for obtaining good chemo- and stereoselectivity. In contrast, C≡C triple bonds are resistant to reduction via transfer hydrogenation.[17]

The asymmetric reduction of the C=N double bond in imines is of great interest for obtaining optically active amines as important building blocks for pharmaceuticals and agrochemicals.[34] In general, imines are best reduced with formic acid-triethylamine, especially when compared to isopropanol, since a moderate rate acceleration can be observed.[17] However, acyclic imines are more difficult to reduce than cyclic ones, usually affording lower yields and ee values. Nonetheless, successful examples for both categories can be found, including 1-subsituted-3,4-dihydroisoquinolines, *N*-sulfonylimines or acyclic ketimines obtained from tetralone and benzylamine.[5,35] However, experimental findings suggest that a slightly different mechanism is operating for the reduction of imines.[36]

## I.4 Alternative Reaction Media – Advantages and Opportunities

Asymmetric transfer hydrogenations are most commonly conducted in either isopropanol or a 5:2 mixture of formic acid-triethylamine. The procedures are well established and many catalysts have shown satisfactory performances with the aforementioned donors and their simultaneous use as solvent.

However, with increasing environmental awareness, the need for greener processes becomes more urgent. Within the 12 principles of green chemistry, the implementation of catalytic rather than stoichiometric transformations is just one important goal. Another one calls for innocuous solvents and auxiliaries,[1] considering the vast amount of solvents used in the chemical industry. In general, it can be said that "the best solvent is no solvent and if a solvent is needed, water is preferred".[3] Water offers many attractive properties as solvent. It is non-toxic, nonflammable and incombustible. In addition, it shows a high heat of evaporation, making it much less volatile than most organic solvents and it is odor- and colorless. Besides, water is one of the most abundant molecules on the planet, hence readily available and inexpensive. Moreover, water can exhibit novel reactivities and selectivities for many transformations, including catalysis. Since many organic compounds are not soluble in water, new reaction concepts are encountered, such as liquid-liquid biphasic catalysis, offering great opportunities, especially for catalyst-product separation when using homogeneous catalysts (see section I.5).[37]

## I.4.1 Effects of Water as Reaction Medium on ATH

Experimental findings in recent years suggest that water has an enormous effect on asymmetric transfer hydrogenations. First of all, reductions performed in water show a dramatic increase in reaction rate compared to the conventional isopropanol or formic acid-triethylamine (TEAF) systems.[29] This might be attributed to the inherent hydrogen bonding ability of $H_2O$. Thereby the hydride delivery could be facilitated due to a more stabilized transition state.[38] Hydrogen bonding is also very likely to facilitate decarboxylation of the formato complex to regenerate the Ru hydride **c**. In addition to that, water as a very polar medium is more suited to stabilize the ionic intermediate formed in the catalytic cycle (see Scheme 7) then isopropanol or TEAF.

Moreover, it has been found that water facilitates the formation of the active catalyst **b** from the precatalyst. When the catalyst is prepared in isopropanol, a base is necessary to generate the active catalyst via abstraction of HCl. However, this formation proceeds in water also in the absence of base, suggesting that water acts as the base for HCl abstraction. This could experimentally be shown, as the reaction solution became acidic upon formation of the active catalyst.[38]

Additionally, the catalyst seems to be much more stable in the presence of water, which can be attributed to the ability of $H_2O$ molecules to coordinate to the Ru metal center, hence being especially able to stabilize the otherwise unsaturated 16 e$^-$ complex **b**. Moreover, the reduction can be controlled by pH adjustment (see I.4.3).[18]

## I.4.2    Adaptations for Aqueous ATH

In order to perform an asymmetric transfer hydrogenation in water and to benefit from the solvent effects, several adaptions of the reaction, including modifications of the hydrogen donor and ligands, are required.

### I.4.2.1    *Hydrogen Donor*

The common donors, isopropanol and formic acid are both soluble in water and can therefore be equally used in an aqueous mixture. However, a third alternative presents itself when switching to water – the salt sodium formate ($HCO_2Na$) can be used as hydrogen donor as well. As a solid, it offers easy handling and operational simplicity. Moreover, it is readily available, cheap, environmentally benign and leads to product formation in an irreversible manner, since $CO_2$ is released as formate is consumed. In addition, it has already been shown that sodium formate in water performs superior compared to aqueous mixtures of isopropanol or TEAF in terms of reaction rates. In 2005, Wu et.al. showed that the asymmetric transfer hydrogenation of acetophenone using the Noyori-Ikariya catalyst with $HCO_2Na$ in water was completed within 1 h with an ee of 94%, whereas the reduction in an aqueous TEAF mixture showed only 2% conversion after 1 h under otherwise similar conditions.[39] This difference can, besides other factors, be attributed to the inherent pH difference when using aqueous $HCO_2Na$ (pH 7) or $HCO_2H$-$NEt_3$ azeotrope in water (pH 3). Another aspect that has to be considered is that the formate ion can only deliver the hydride for the reduction of a ketone. The proton has to be contributed from a water molecule. Keeping this in mind, the mechanism for regenerating the hydrido complex **c** with $HCO_2Na$ can be formulated in analogy to the regeneration mechanism with formic acid (see Scheme 6).

### I.4.2.2    *Catalyst*

In many publications, unmodified ATH catalysts, such as the Noyori-Ikariya catalyst, have been successfully employed for the reduction of ketone substrates in aqueous solutions using sodium formate. In the experiments, the precatalysts seemed to be water soluble, although with varying degrees.[18] In general, rhodium and iridium based catalysts show a greater water solubility compared to ruthenium analogues. Presumably, their water solubility stems from a ligand exchange in the aqueous medium, where the chloride is replaced by a water molecule, forming a monoaqua complex. Nevertheless, the solubility of those unmodified catalysts is still higher in the organic substrate/alcohol than in water. Since most organic substrates are not soluble in water, a biphasic reaction mixture will form, with the catalyst preferentially residing in the organic phase, whereas the hydrogen donor sodium formate will still be in the aqueous phase. Surprisingly, this does not directly inhibit the successful reduction of ketones, since experimental results proof the feasibility of this reaction setup. It can therefore be assumed that the catalysis is taking place "on water".[18]

However, the preferential solubility of the catalyst in the organic product phase causes problems for efficient catalyst-product separation. This is a critical point for many transition metal based reactions, since the catalysts are often very expensive and metal residues in the final product should be avoided. Consequently, great effort has been put into designing water soluble catalysts by synthesizing water soluble ligands as discussed in chapter I.5 in detail

## I.4.3    Mechanistic Aspects and pH Dependency

As mentioned earlier, water has a dramatic influence on various aspects of asymmetric transfer hydrogenations. The largest effect is that water alters the mechanism of the catalytic process. This stems not only from its polar nature, which supports an ionic mechanism, but also from the pH dependency of the actual operating pathway. A pH dependency in aqueous ATH was first observed by Ogo et.al. in 2002.[40] They concluded that the optimal pH range is dependent on the $pK_a$ value of the hydrogen donor ($pK_a$ of $HCO_2H$ = 3.6) and the aqua complex existing in water ($pK_a$ between 7-8), thus a general pH range between 5-8 can be assumed as ideal.[39] The possible alterations concerning the reaction pathway depending on the solution pH are depicted in Scheme 8 and are discussed below.

Scheme 8. pH dependency in aqueous ATH
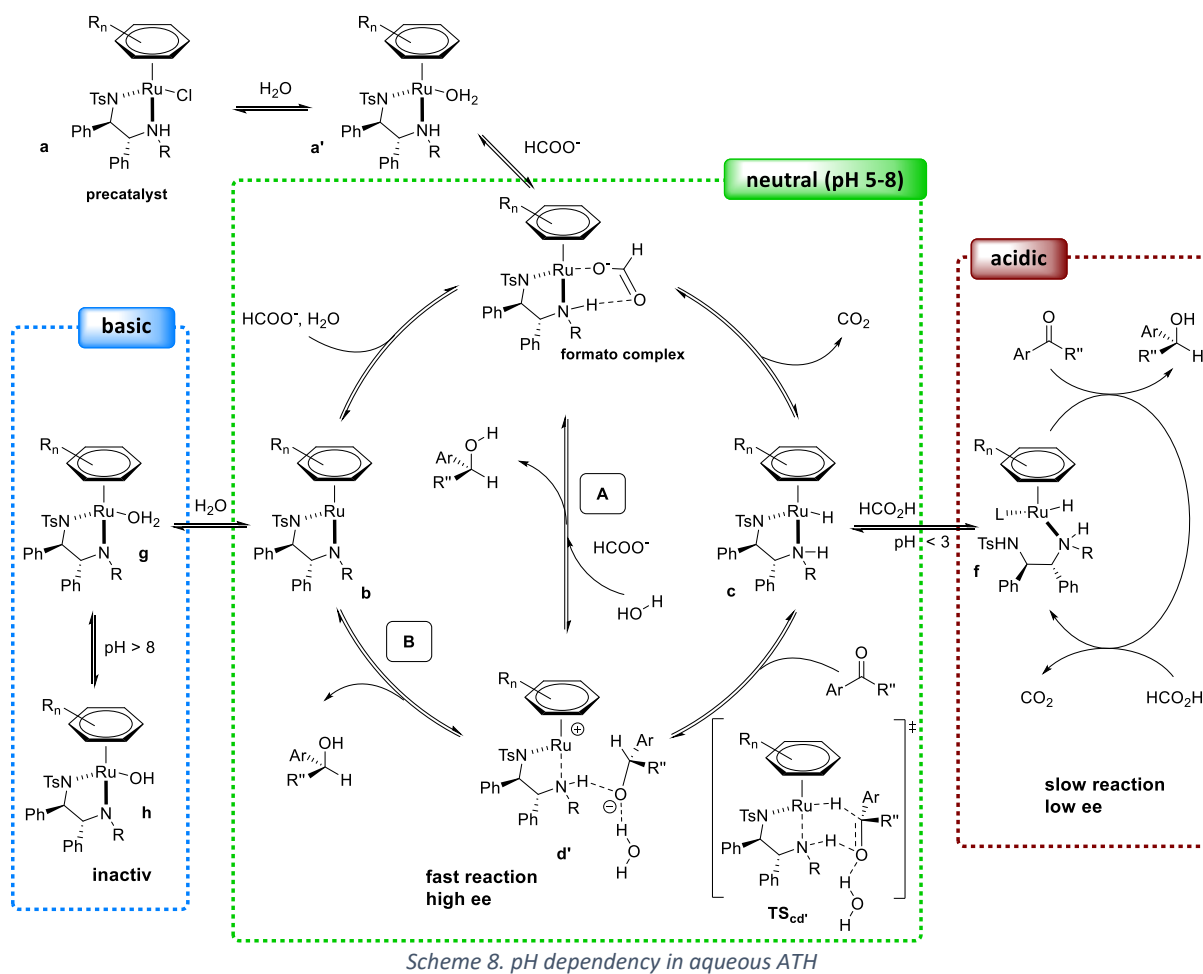
<u>Low pH</u>

At a pH below 3.6 formic acid exist mostly in its protonated form. Therefore, the concentration of formate ions, which are required to form the corresponding Ru formato complex to regenerate the hydride is very low, resulting in a very slow reaction. This explains the initially observed slow reaction in TEAF. In the beginning, the solution pH value is 3, so the formate concentration is very low. Only with time, when $HCO_2H$ is slowly consumed in the ketone reduction, the pH starts to rise, leading to a sharp increase in TOF (turn over frequency) once a pH of 4 is reached. In addition to this pH dependent reaction rate, a decrease in enantioselectivity at low pH values could be observed,[39] suggesting that under acidic conditions a competing pathway might be operating (see Scheme 8). It has been proposed and supported by experimental and computational results that the coordinated Tsdpen ligand is protonated at the amido nitrogen under such conditions, leading to dissociation from the Ru center.[38,39] The former bidentate ligand remains only coordinated via one nitrogen atom. Consequently, the transition state in the reducing step is far less ordered, leading to a decrease in enantioselectivity.

High pH

At pH values above 8 another effect becomes noticeable. In general, the formation of aqua complexes of the corresponding catalyst in water is a reversible process, implying that the $H_2O$ ligand can again be replaced e.g. by a formate ion. However, at rising pH values the $H_2O$ ligand is transformed into a hydroxyl group. The formed hydroxo complex is far more stable, so the formate ion is no longer able to coordinate to the complex by replacement of the hydroxyl ligand, making the hydroxo complex inactive in ATH. Thus, the observed decrease in reaction rate at high pH can be explained.[38]

Neutral pH

Due to the effects occurring at low and high pH, it is crucial for the success of aqueous ATH to maintain a pH value in the range of approximately 5-8 throughout the reaction. In this pH region, the catalytic cycle in Scheme 8 follows the one already shown in Scheme 7. At first, the monoaqua complex **a'** will form by ligand exchange from the precatalyst **a**. Subsequent displacement by a formate ion yields the formato complex. After decarboxylation, the obtained Ru hydrido complex **c** can react with the ketone substrate. Additional water molecules will stabilize the transition state **TScd'** by forming hydrogen bonds. These hydrogen bonds will also have a stabilizing effect on the intermediate ion pair **d'**, from which the reduced alcohol can be obtained either by proton transfer from the ligand (**B**), or more likely by proton transfer from a water molecule (**A**).

## I.5    Catalyst Immobilization

In the last sections, the achievements in the field of asymmetric transfer hydrogenation have been pointed out. However, as is the case with every process involving homogeneous catalysts, it suffers from the major drawback of cumbersome catalyst separation and recycling. Therefore, many attempts in catalyst design have been aiming at immobilizing the catalyst in one way or another. In principle, immobilization can be achieved either via a heterogeneous or a homogeneous catalysis approach (Figure 10).
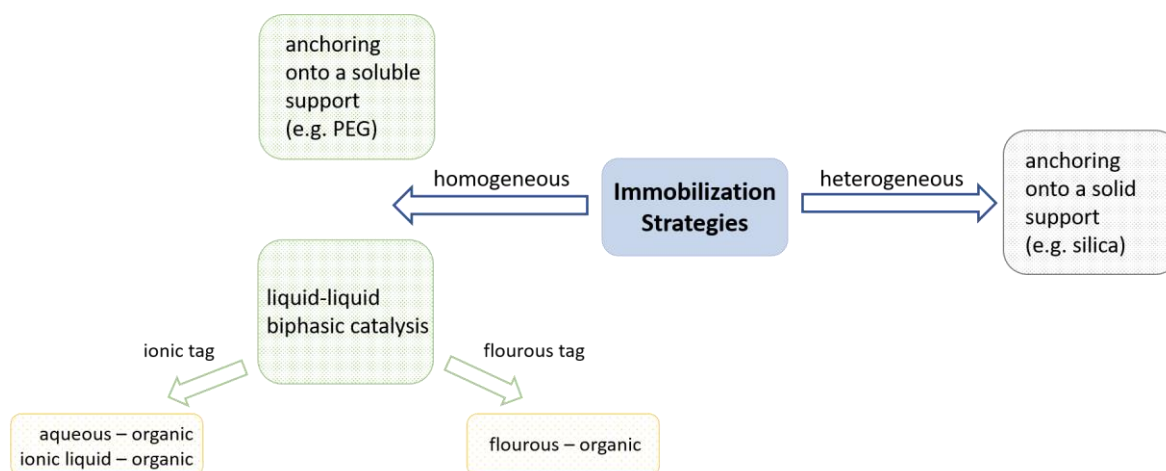


*Figure 10. Catalyst immobilization strategies in homogeneous catalysis*

Heterogenous immobilization strategies

A heterogeneous immobilization approach is to heterogenize the homogeneous catalyst by anchoring it onto a solid support, either by covalent bonding (e.g. grafting the ligand onto silica or an insoluble polymer) or non-covalent interactions. Obviously, the catalyst separation could then be achieved by simple filtration, thereby also providing ideal conditions for a continuous reaction set-up in an immobilized catalyst cartridge. However, these attempts to bind the catalyst often suffer from reduced catalyst activity and/or selectivity, metal leaching and degradation of the support material.[3]

Homogeneous immobilization strategies

To immobilize the catalyst in a homogeneous fashion, different approaches are possible. On the one hand, the catalyst can be covalently bond to a soluble polymer, such as PEG (polyethylene glycol). On the other hand, the catalyst can be immobilized by dissolving it in a liquid phase that is immiscible with the product phase. This concept is known as liquid-liquid biphasic catalysis. The catalyst can then be separated, and ideally reused, by simple phase separation of the two liquids and addition of a fresh batch of reactants. This concept has become particularly
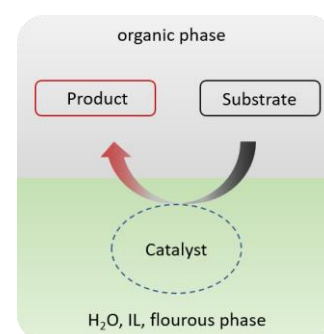


*Figure 11. Concept of liquid-liquid biphasic catalysis*

interesting in combination with the use of alternative solvents, such as water, ionic liquids (ILs) or fluorous solvents as the catalyst dissolving phase. They are immiscible with common organic solvents, or most organic reagents, so that a biphasic mixture as depicted in Figure 11 can be obtained.

As key requirement for this strategy, the catalyst has to be modified in such a way that it cannot only be dissolved in the aqueous, ionic liquid or fluorous phase, but also remains in this phase while the products form a separate, immiscible organic phase. Modification strategies therefore include either "ionization" of the ligands to make the catalyst soluble in water or ionic liquids, or to attach a fluorous tag to the ligand, if a fluorous solvent is used.

With respect to asymmetric transfer hydrogenations, aqueous biphasic catalysis is probably the most advantageous immobilization strategy out of the aforementioned ones. On the one hand, water readily separates from organic solvents forming a biphasic mixture. On the other hand, water offers a greener reaction setup and enhanced reactivity, owing to its unique properties. Most importantly, water offers an ideal reaction environment for the use of sodium formate as non-reversible hydrogen donor which is only sparingly soluble in common organic solvents.

In an aqueous biphasic reaction setup, the catalyst and the hydrogen donor will be dissolved in the aqueous phase, while the substrates and products are forming a separate organic phase, as they are usually insoluble in water. To successfully immobilize the catalyst in the aqueous phase, the polarity of the catalyst has to be increased, ideally via introduction of very polar or charged groups. Some of those modification strategies have already been applied to a variety of ligand motives, including the Noyori-Ikariya catalyst and are exemplified in Figure 12.
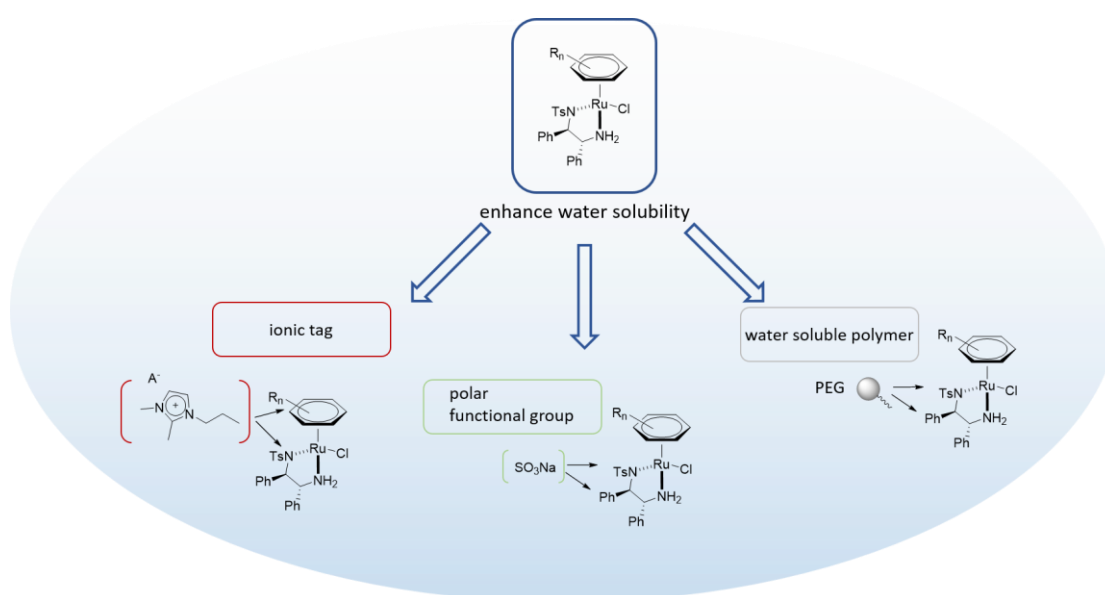


*Figure 12. Modified Noyori-Ikariya catalysts for enhanced water solubility*

One possibility is to introduce a polar or ionic functional group such as a sulfonate group, either at the phenyl substituents of the chiral diamine ligand or at the tosyl group. Another option is to attach an ionic subunit to the ligands, such as an imidazolium tag, making the catalyst water soluble as well. Furthermore, binding the catalyst to a PEG unit also results in water solubility, representing a combination of the two homogeneous immobilization strategies shown in Figure 10.[17,39] While these strategies could efficiently immobilize the Ruthenium catalyst in the aqueous layer, considerable synthetic effort over multiple steps, often in combination with chromatographic separation of isomers was typically required to obtain the desired functionalized ligands.

To further circumvent the problem of the low water solubility of most substrates, surfactants can be used, yielding better results than obtained for reductions performed without.[41] In recent years, successful examples of the combination of both approaches in one molecule have also been reported.[42] By introducing a long alkyl chain into the ligand in combination with an ionic group, a surfactant-like catalyst can be obtained, especially facilitating the reduction of long chain aliphatic ketones.

Based on these novel developments, there have already been successful examples of asymmetric transfer hydrogenations run in aqueous biphasic systems on large scale. One example is the reduction of various ketones with the water soluble, chiral Csdpen complex of Ru, Rh or Ir (Csdpen = *N*-camphorsulfonyl-1,2-diphenylethylendiamine), depicted in Figure 13, yielding the chiral alcohols in excellent ee values and at fast rates. This process has even been used on a > 100 kg scale to produce a wide range of chiral alcohols from the corresponding ketones with high selectivity and efficiency.[7]
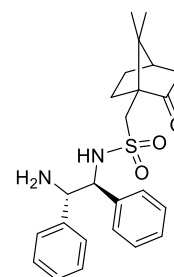


*Figure 13. Csdpen ligand*

## II   Aim of Thesis

The stereoselective reduction of carbonyls to chiral secondary alcohols plays an important role in asymmetric synthesis. Among various methods, catalytic transfer hydrogenations provide an attractive strategy. The reduction of multiple bonds can be achieved with the aid of a catalyst using small organic molecules as hydrogen donor. In case of transition metal catalyzed asymmetric transfer hydrogenations, chiral β-amino alcohols or chiral diamines are considered the most efficient ligands.
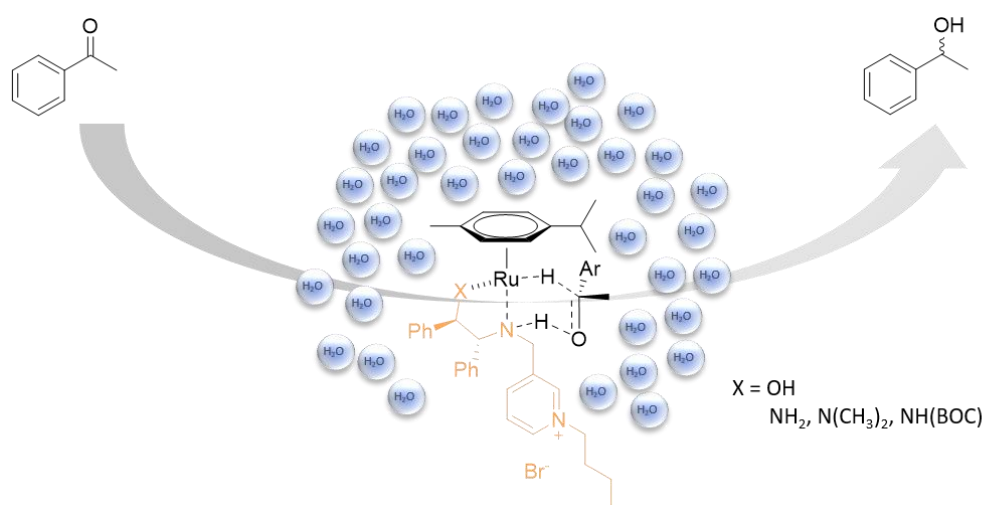


*Figure 14. Graphical abstract for aqueous asymmetric transfer hydrogenation*

In this thesis, the design and synthesis of coordinating chiral ionic ligands should be investigated for the application in the asymmetric transfer hydrogenation of aromatic ketones in water. Based on the preliminary results obtained with chiral β-amino alcohols as chiral ligands, the ligand scope should be further expanded to chiral diamines. Moreover, the substrate scope for the developed catalyst system should be examined.

# III  Results and Discussion

## III.1   Design and Synthesis of Chiral Ionic Ligands for ATH

For a successful application in aqueous asymmetric transfer hydrogenation, a ligand has to meet the following basic requirements:

- Bidentate ligand structure for coordination to the metal center
- Sterically demanding chiral backbone for chiral induction
- Primary / secondary amine functionality to enable the transition state
- Additional ionic functionality to tune catalyst solubility

Following these prerequisites, a chiral *O,N* and *N,N* structural motive was chosen as bidentate ligand. To ensure sufficient water solubility for the active catalyst complex, an ionic subunit was attached to the ligand. For this purpose, a pyridinium head group was selected. A critical point favoring a pyridinium group over commonly employed ammonium groups is the commercial availability and stability of pyridine-3-carboxaldehyde as precursor. Moreover, using a pyridinium head group avoids the presence of acidic protons, which are found in common imidazolium cations and can have an unpredictable influence on transition metal catalyzed reactions due to carbene formation.[43] Quaternization of the ligand precursor is performed with an alkyl halide to yield the desired chiral ionic ligand with a cationic pyridinium head group. Considering these aspects, the following, general synthesis strategy was proposed (Figure 15).
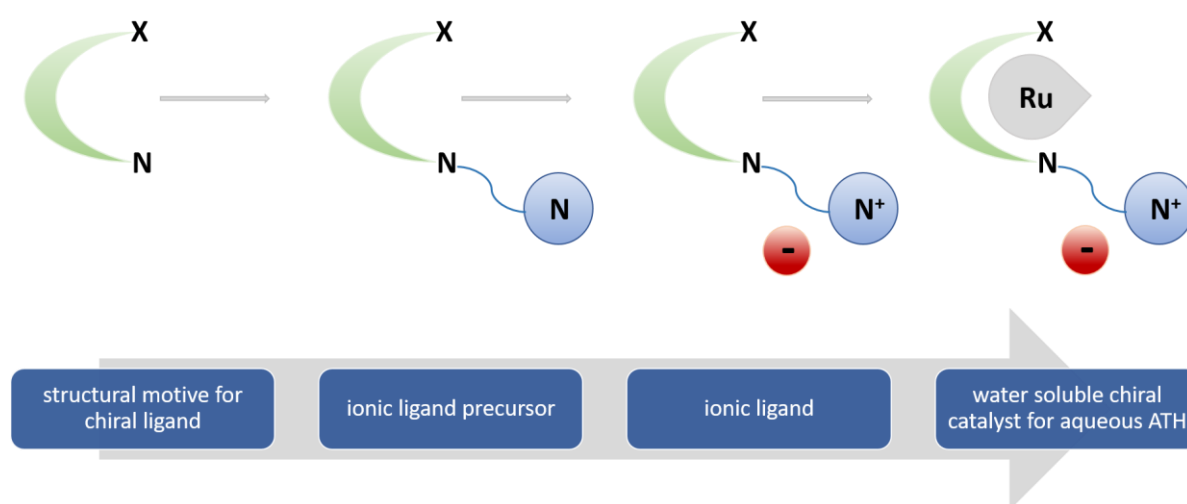


*Figure 15. General synthesis strategy for chiral ionic ligands*

Based on the structural motive of common ATH ligands, particularly the Noyori-Ikariya catalyst, (1*S*,2*R*)-2-amino-1,2-diphenylethanol and (1*R*,2*R*)-1,2-diphenylethylenediamine were chosen as bidentate ligand motives. By grafting pyridine-3-carboxaldehyde onto the chiral backbone, the ionic

ligand precursor could be obtained. Selective alkylation with *n*-butyl bromide of the pyridine nitrogen yielded the ionic ligand. By choosing bromide as counterion, a highly water soluble, chiral ionic ligand could be obtained (Figure 16). The synthesis of the desired ligands will be discussed in more detail in the following sections.
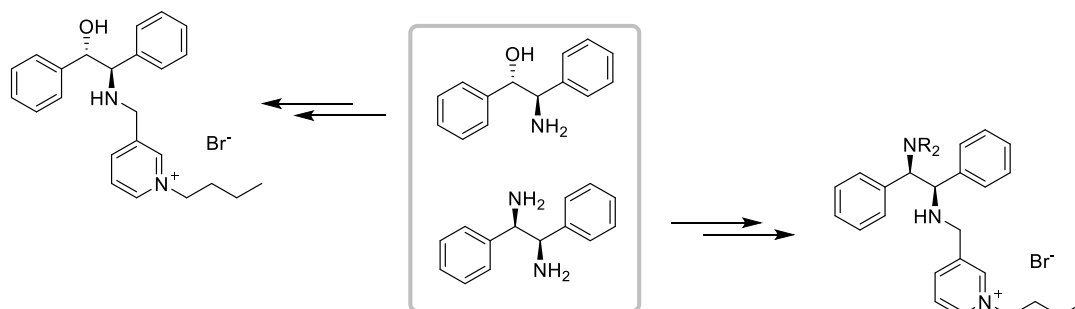


*Figure 16. Overview of the chosen bidentate ligand motives and the desired chiral ionic ligands*

## III.1.1    Synthesis of Amino Alcohol based Chiral Ionic Ligands

Based on the preliminary work by Maria Vasiloiu,[43] the desired hydrophilic, chiral ionic ligand **3** could be obtained in two steps starting from commercially available chiral amino alcohol **1**. The ligand precursor was synthesized by reductive amination with pyridine-3-carboxaldehyde and subsequent reduction with sodium borohydride. Selective alkylation of the pyridine nitrogen with *n*-butyl bromide gave the desired ligand **3** in high overall yield as depicted in Scheme 9.
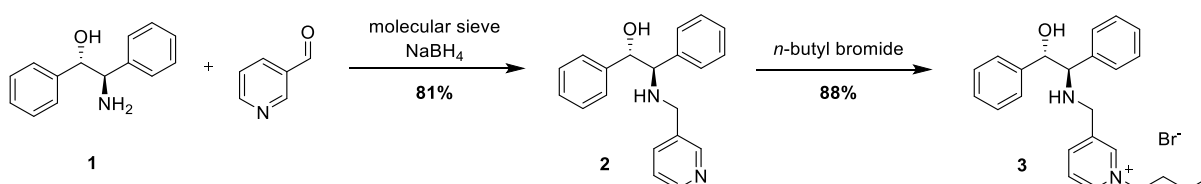


*Scheme 9. Synthesis of amino alcohol based chiral ionic ligand 3*

Having a pyridine nitrogen and a secondary amine functionality in the same molecule, two potential alkylation sites are present. Consequently, selective alkylation of the pyridine nitrogen is the key challenge in this synthesis. Using 1.2 equivalents *n*-butyl bromide at 80 °C led to the preferred alkylation of the pyridine nitrogen. Under these conditions, no double alkylation could be observed, which is in contrast to what was previously reported by Vasiloiu et. al.[43] Hence, ligand **3** could be obtained in high purity and was used without further purification.

To investigate the influence of the ligand stereochemistry on activity and selectivity in asymmetric transfer hydrogenation, as well as to be able to directly compare the analogues diamine and amino alcohol ligands, a small batch of (1*R*,2*R*)-2-amino-1,2-diphenylethanol based ionic ligand was also

synthesized. Following the synthesis protocol employed above, ligand **6** could be obtained in high overall yield as shown in Scheme 10.
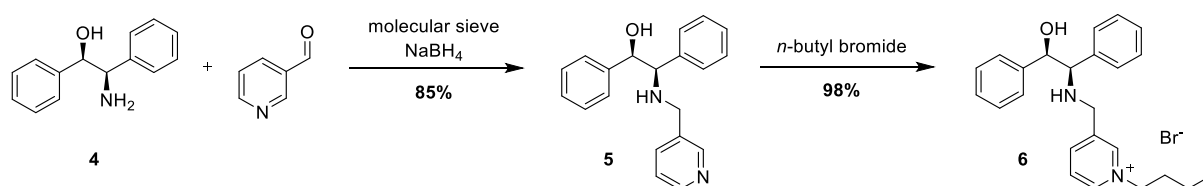


*Scheme 10. Synthesis of amino alcohol based chiral ionic ligand with (R,R) configuration*

## III.1.2 Synthesis of Diamine based Chiral Ionic Ligands

Chiral diamine ligands have shown great activities and selectivities in asymmetric transfer hydrogenations, with *N*-(*p*-toluenesulfonyl)-1,2-diphenylethylenediamine (Tsdpen) in the Noyori-Ikariya catalyst being the standard reference to evaluate the performance of new ligands. Hence, the above developed concept of a hydrophilic ionic ligand was also applied to a chiral diamine. For this purpose, commercially available (1*R*,2*R*)-1,2-diphenylethylenediamine (dpen) was chosen as the structural motive. This allowed for the direct comparison with the analogue amino alcohols **3** and **6** as well as the structurally similar Tsdpen ligand (see Figure 17).
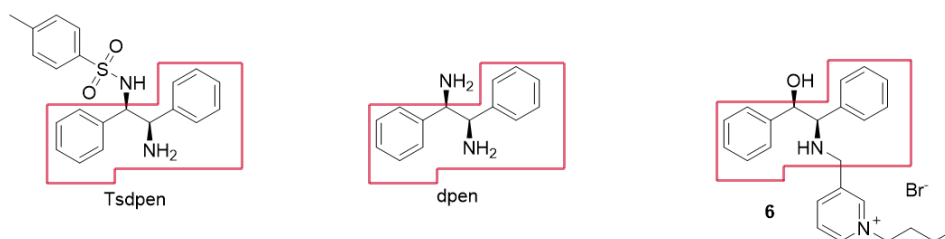


*Figure 17. Structural similarities between the chosen ligand motives and Tsdpen*

Furthermore, different substitution patterns on one amine functionality were exploited. For this purpose, a primary amine functionality (**16**), a dimethylated tertiary amine functionality (**12**) and a BOC protected amine functionality (**15**) (BOC = *tert*-butyloxycarbonyl) were established, resulting in the final ligands depicted below. Additionally, they all share the necessary secondary amine functionality to participate in the transition state in ATH and the cationic pyridinium head group to enhance water solubility of the final catalyst. These similarities also allow for the direct comparison with amino alcohol based chiral ionic ligand (CIL) **3**.
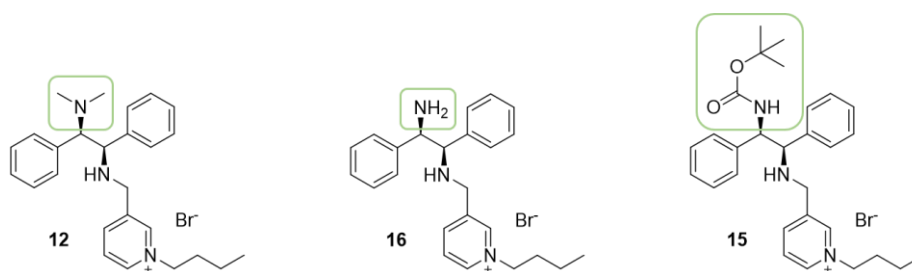
*Figure 18. Synthesized diamine based chiral ionic ligands with different substitution patterns*

As two equally reactive primary amine functionalities are present in the starting dpen molecule, the use of protecting groups to achieve selective reaction at only one of those groups could not be avoided. For this purpose, a phthaloyl and a BOC protecting group were chosen. Their properties are compared in Table 2. As can be seen protection and deprotection of the two groups are done under opposite conditions, allowing for the proper choice in adaptation to the planed reaction conditions. Both groups are stable towards most nucleophiles and bases and also in a wide pH range in aqueous solutions. A big advantage of the phthaloyl group is that deprotection with hydrazine can be achieved under mild and near-neutral conditions in a highly selective fashion.

*Table 2. Comparison of phthaloyl vs. BOC protecting group*

| protecting group | Phthaloyl  | BOC  |
|---|---|---|
| **protection** | dehydrative condensation of phthalic anhydride under **acidic** conditions | reaction with anhydride $(BOC)_2O$ under **basic** conditions, usually anhydrous |
| **deprotection** | most common **hydrazinolysis**, also basic hydrolysis | under anhydrous, **acidic** conditions |
| **stability** | stable towards most nucleophiles and bases | stable towards most nucleophiles and bases |
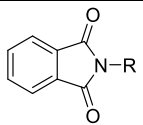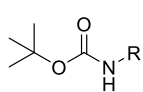
Nonetheless, the use of protecting groups resulted in additional steps that had to be included in the general synthesis strategy developed above. Moreover, as ionic compounds are generally difficult to purify via conventional methods, such as column chromatography or distillation, it is important to establish the quaternization step as late as possible in the reaction sequence. Therefore, the selective functionalization of the highlighted amine functionality in Figure 18 was usually done before the subsequent reductive amination and alkylation step.

### III.1.2.1  *Synthesis using a Phthaloyl Protecting Group*

Employing a phthaloyl group as protecting group offers some advantages. It selectively protects only one of the two available amine functionalities and deprotection can be achieved under mild conditions. Moreover, it is stable towards a variety of reagents, allowing for diverse transformations to be performed whilst retaining the protecting group.

Displaying these advantageous properties, a phthaloyl protecting group was chosen for the synthesis of the dimethylated diamine ligand **12**. Selective protection of dpen (**7**) was achieved using phthalic anhydride under acidic, anhydrous conditions. Subsequent dimethylation, following the Eschweiler-Clarke procedure using formaldehyde and formic acid yielded the tertiary amine. Deprotection with hydrazine gave intermediate **10** in overall high yields.
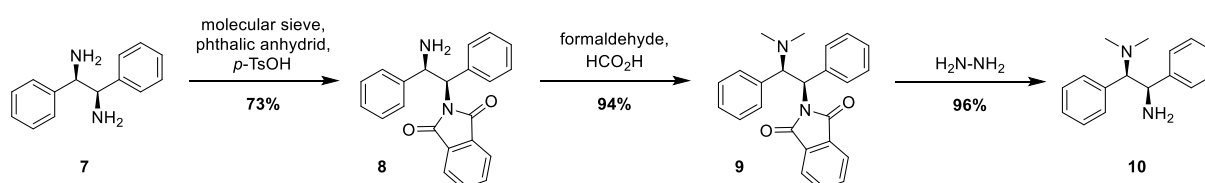


*Scheme 11. Selective dimethylation of dpen using a phthaloyl protecting group*

As the obtained tertiary amine functionality is not able to participate in the reductive amination with pyridine-3-carboxaldehyde, no additional modifications were necessary. Consequently, **10** could be transformed into the final ionic ligand following the two-step procedure already established for the synthesis of amino alcohol based ligands (see III.1.1). Hence, chiral ionic ligand **12** could be obtained in high overall yield. Again, no double alkylation was observed and the crude ligand could be used without further purification.
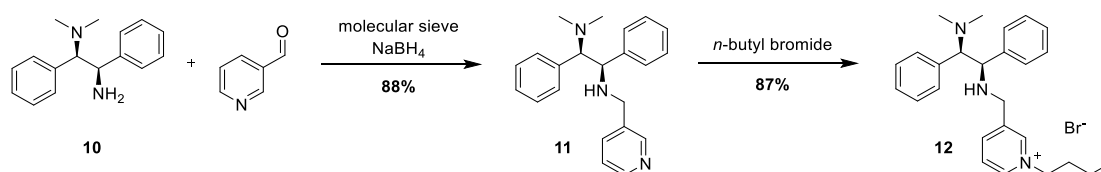


*Scheme 12. Synthesis towards chiral ionic ligand 12*

As the protection - deprotection sequence using a phthaloyl protecting group presented no difficulties, it was obvious to apply it to the synthesis of chiral ionic ligand **16** as well. As the primary amine functionality would most likely also be alkylated to a great degree in the quaternization step, it would be necessary to establish the deprotection at the end of the synthesis sequence. Considering this, the following reaction sequence was proposed (see Scheme 13).
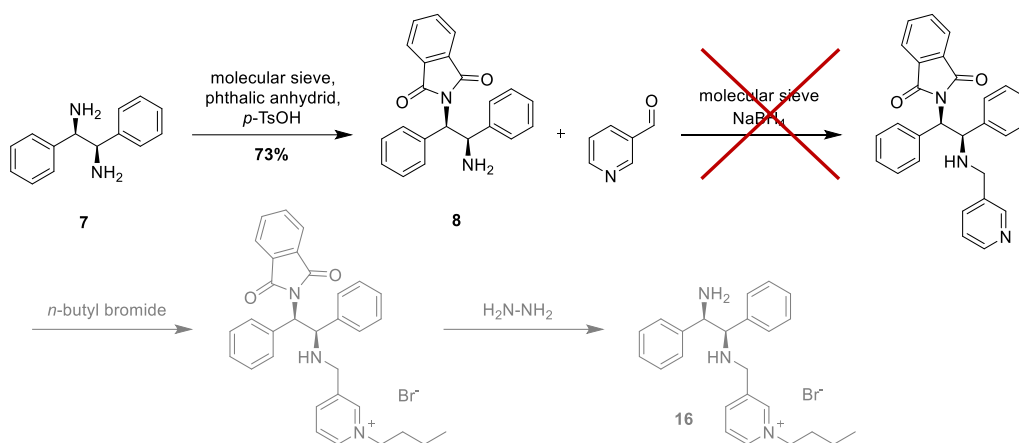
*Scheme 13. Originally proposed synthesis towards chiral ionic ligand 16*

However, the reductive amination of **8** under the given conditions (1.0 equiv. freshly distilled pyridine-3-carboxaldehyde, anhydrous methanol and molecular sieve, refluxing overnight) was not possible. Meticulous monitoring of the reaction progress via TLC from the beginning did not show any conversion, even after prolonged reaction time or increasing the amount of pyridine-3-carboxaldehyde. The attempt to isolate the imine intermediate was also unsuccessful, as only starting material could be recovered. Furthermore, upon addition of sodium borohydride, only partial cleavage of the phthaloyl group via ring opening and reduction of the aldehyde as depicted in Scheme 14 could be observed. These results indicate that the phthaloyl group has an inhibiting effect on this reaction. Therefore, an alternative synthesis route towards CIL **16** had to be developed.
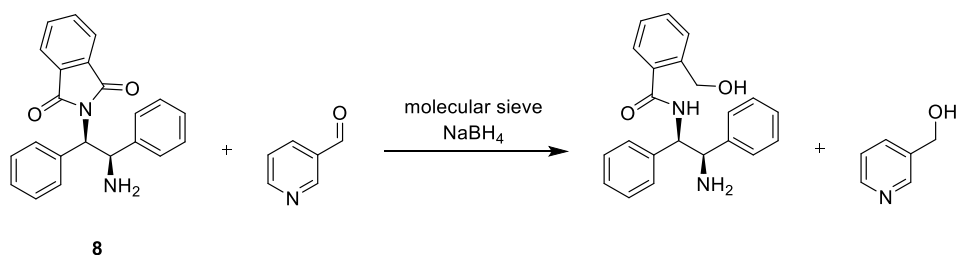


*Scheme 14. Partial reductive ring opening of phthaloyl protecting group with sodium borohydride*

### III.1.2.2  *Synthesis using a BOC Protecting Group*

As alternative to the phthaloyl protecting group, a BOC group was chosen. In contrast, selective mono protection using a BOC protecting group is not easily achievable, since a mono protected and unprotected diamine molecule are equally reactive towards the reaction with di-*tert*-butyl dicarbonate (BOC)$_2$O. Therefore, a selective synthesis had to be developed. By adapting a literature protocol,[44] which reported the successful mono BOC protection under unusual acidic conditions, a viable route to the mono BOC protected diamine **13** could be established.
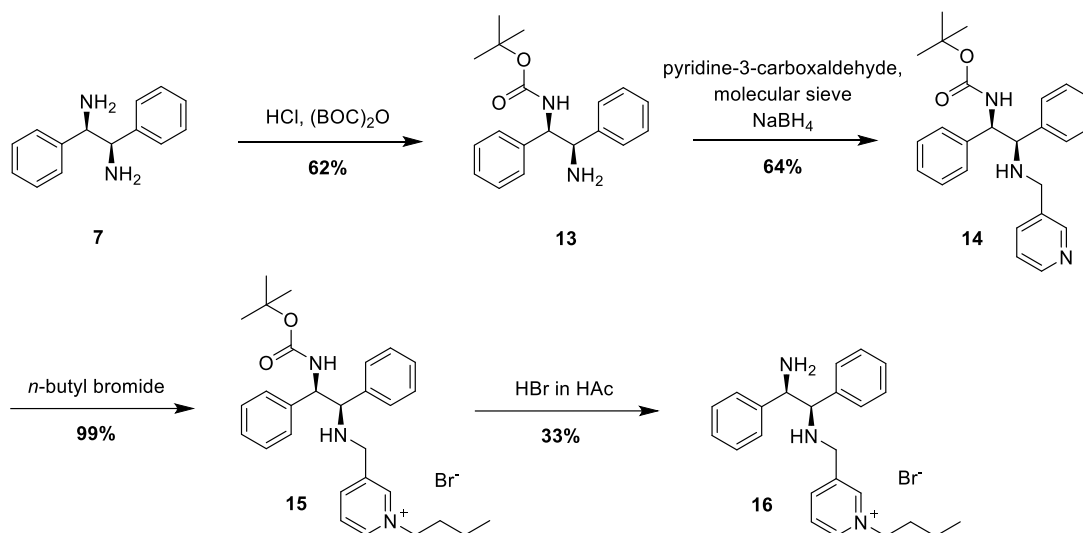
*Scheme 15. Synthesis towards chiral ionic ligand 15 and 16 using a BOC protecting group*

Subsequently, the general, two step synthesis protocol towards the final ligand could be applied. Reductive amination with pyridine-3-carboxaldehyde and subsequent reduction with sodium borohydride gave the ionic ligand precursor **14**. However, only lower yields could be obtained, compared to the other ligand precursors **2**, **5** and **11**. The following alkylation step with *n*-butyl bromide gave the desired ionic ligand **15** in excellent yield. Again, selective alkylation at the pyridine nitrogen was observed. For obtaining the free amine functionality in chiral ionic ligand **16**, the deprotection step had to be done after the quaternization reaction, to avoid double alkylation at the reactive primary amine functionality. For deprotection, a standard protocol using HBr in concentrated acetic acid was followed. Although the reaction itself proceeded fine with a crude yield of approximately 80%, some difficulties during the work up and subsequent purification were encountered. To isolate the product quantitatively from the aqueous reaction mixture after neutralization, many extraction steps with dichloromethane were necessary, since the ionic ligand was equally soluble in both phases. Moreover, the crude product was not pure enough to be used directly. Purification could be achieved via column chromatography using a mixture of EtOH, $H_2O$ and acetic acid as mobile phase with silica as stationary phase. However, loss of product during the chromatography step could not be avoided. Additionally, it was not possible to fully remove acetic acid under reduced pressure, as a highly viscous glass was formed and no heat could be applied during the drying process to avoid deterioration of the stereogenic centers. Hence, an aqueous work up to neutralize the acetic acid and subsequent extraction of the product with $CH_2Cl_2$ as before was alternatively tried. However, quantitative extraction was again difficult. Due to these problems encountered during work up and purification, the final ligand **16** could only be isolated in 33% yield.

## III.2   Application of Chiral Ionic Ligands in Aqueous ATH

To evaluate the newly designed, hydrophilic, chiral ionic ligands, their performance in the Ru-catalyzed asymmetric transfer hydrogenation in aqueous medium was investigated. The reduction of acetophenone to 1-phenylethanol was chosen as test reaction, using sodium formate as hydrogen donor and [Ru($p$-cymene)Cl$_2$]$_2$ as catalyst precursor (Scheme 16). Due to the air sensitivity of the active catalyst, the reactions had to be conducted under inert atmosphere and the water purged with argon prior to use.
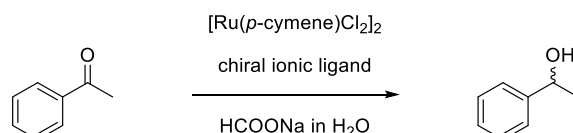


*Scheme 16. Reduction of acetophenone to 1-phenylethanol in aqueous ATH*

Based on the conditions already established for amino alcohol based ligands by Vasiloiu,[43] the new diamine ligands were initially tested at 40 °C for 24 h and 48 h and compared to the results for CIL **3**. The results are depicted in Figure 19 and Figure 20 below.
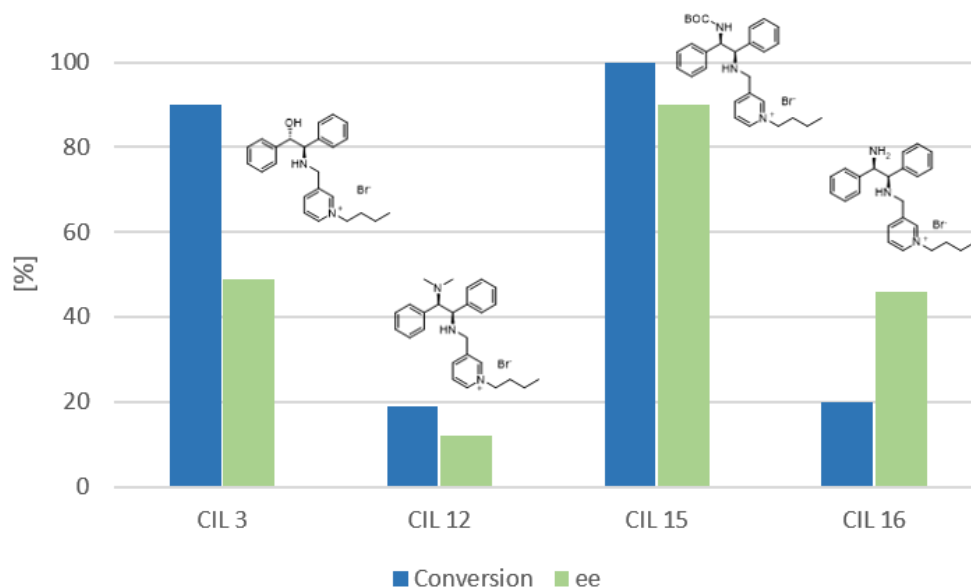


*Figure 19. Aqueous ATH performed with chiral ionic ligands at 40 °C for 24 h*

*Performed with 2 mmol ketone, 10 mmol HCO$_2$Na, 0.5 mol% [Ru(p-cymene)Cl$_2$]$_2$ and 1.05 mol% CIL in 4 mL H$_2$O. Conversion determined by HPLC analysis. Enantiomeric excess determined by HPLC analysis using a DAICEL Chiralcel IB column.*
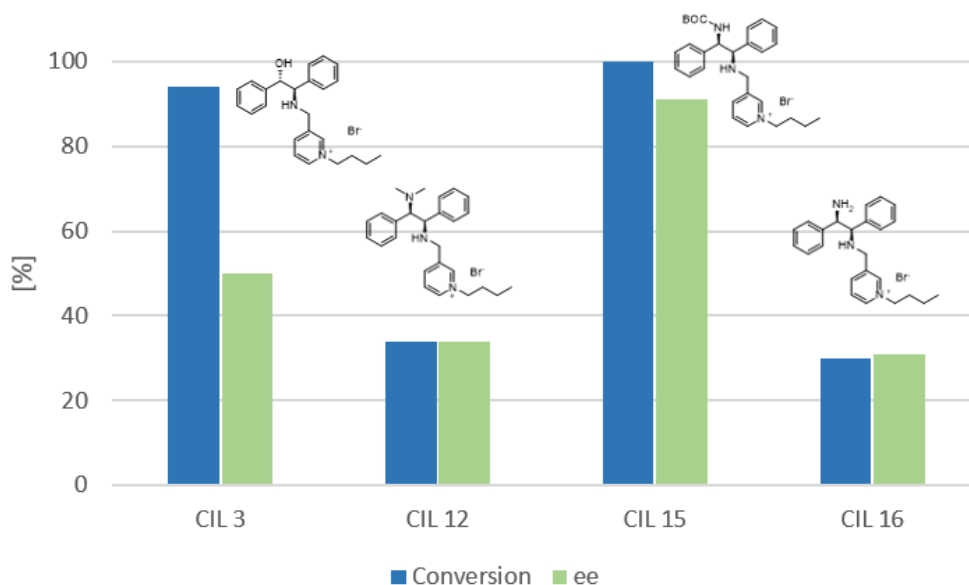
*Figure 20. Aqueous ATH performed with chiral ionic ligands at 40 °C for 48 h*

*Performed with 2 mmol ketone, 10 mmol HCO$_2$Na, 0.5 mol% [Ru(p-cymene)Cl$_2$]$_2$ and 1.05 mol% CIL in 4 mL H$_2$O. Conversion determined by HPLC analysis. Enantiomeric excess determined by HPLC analysis using a DAICEL Chiralcel IB column.*

The results show that BOC protected CIL **15** performed best, giving full conversion already after 24 h and excellent ee values of 90%. As expected, the amino alcohol based ligand **3** also showed high activity, resulting in almost full conversion after 24 h. However, the ee values are significantly lower and only 50% enantiomeric excess were obtained. The other two diamine based CILs **12** and **16** both performed poorly. Although an increase in conversion could be observed on extending the reaction time from 24 h to 48 h, the obtained values did not exceed 35%. In addition, enantioselectivities were also low. Only CIL **16** showed comparable selectivity to CIL **3** after 24 h. Another interesting finding is the inverted stereochemistry for CIL **12** compared to CIL **15** and **16** as shown in Table 3, considering that all three ligands share the same stereochemistry. Based on these results the following observations concerning the ligand design and properties could be made.

*Table 3. Overview on CIL stereochemistry vs product stereochemistry*



| CIL | 3 | 6 | 12 | 15 | 16 |
|---|---|---|---|---|---|
| Product configuration | (S) | (R) | (S) | (R) | (R) |

Influence of substitution pattern

Comparing CIL **12** with the other ligands suggests that the two methyl groups on the tertiary amine are hindering a good coordination to the metal center. For CILs **3**, **15** and **16** coordination can be facilitated by the abstraction of a proton from either the −OH (**3**), −NH−BOC (**15**) or −NH$_2$ (**16**) moiety. Thus, the catalyst formed with CIL **12** probably shows a rather distorted complex geometry, leading to a less stable catalyst complex, hence resulting in poor activity and selectivity.



X = O; N(CH$_3$)$_2$; NH; N(BOC);

*Figure 21. Ru based catalyst structure with synthesized chiral ionic ligands*

Another aspect to be considered is the formed complex diastereomer. In general, two diastereomers can be formed in regard of the Ru center upon ligand coordination (Figure 22). For diamine ligands with (*R*,*R*) configuration, such as CIL **15** and **16** it seems that the (*S*)-diastereomer is preferentially formed, leading to the (*R*) product isomer. However, dimethylation of the ligand seems to distort the catalyst geometry in such a way that the opposite diastereomer becomes the more favorable one. Hence, the opposite stereo induction for the product formation can be observed, with CIL **12** leading to the preferred formation of the (*S*)-enantiomer of 1-phenylethanol. This inversion of product stereochemistry due to full alkylation has already been suggested in literature by Dub and Gordon.[9]



minor diastereomer

major diastereomer
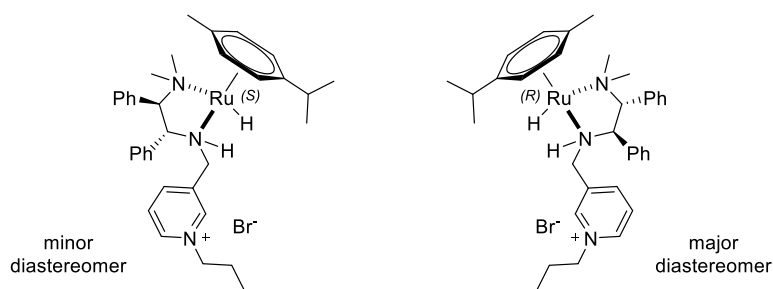
*Figure 22. Diastereomers formed from Ru-precursor and CIL 12*

Influence of electron density

The difference in activity of CIL **3** and **15** compared to **16** might be explained by taking a closer look at the electron density at the involved heteroatoms (Figure 23)[1]. The estimated values for CIL **3** and **15** are rather similar, whereas the electron densities at *N2* and *N3* in CIL **16** deviate from these values. Considering the results obtained above, this would suggest that an electron density around -0.7 would be ideal. Heteroatoms displaying a higher negativity might already be too basic to deliver a proton to the substrate in the transition state, assuming that *N3* is involved in it. On the other hand, if *N2* takes part in the transition state, a lower electron density might suggest that the nitrogen atom is not basic

---

[1] Electron densities were calculated by Veronika Zeindlhofer, BSc and Assoz. Prof. Dipl.-Chem. Dr. Christian Schröder from the Department of Computational Biological Chemistry at the University of Vienna, 1090 Wien.

enough to regenerate the NH functionality in the catalytic cycle by abstraction of a proton from the solvent (see I.3.2.2). Either effect would lead to a decrease in reaction rate, being a possible explanation for the low conversion observed for CIL **16**. It could also be argued that the high value at *N3* prevents a good coordination to the metal center since proton abstraction would be more difficult. However, compared to the two methyl groups in CIL **12**, the small H-atoms should nonetheless enable a sufficient coordination. This could be supported by the decent ee values obtainable with CIL **16** and the preferred formation of (*R*)-1-phenylethanol.
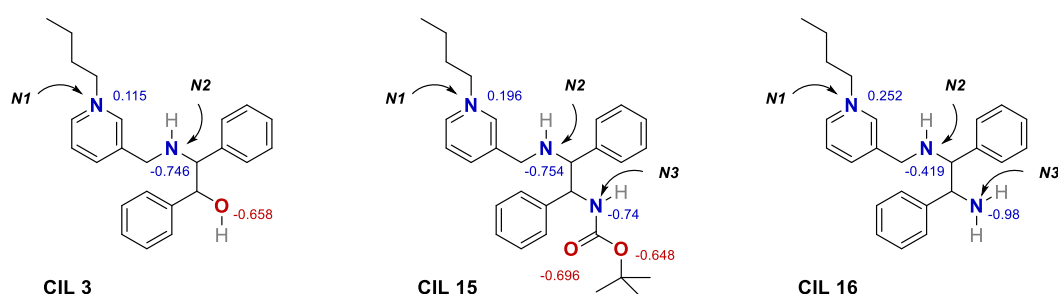


*Figure 23. Calculated electron densities for CIL 3, 15 and 16. Charges in water (PCM method) were fitted using the CHelpG scheme and the !B97XD functional with an augmented cc-pVDZ basis set*

Factors influencing enantioselectivity

Concerning the enantioselectivity, it seems that the ionic head group does not influence the stereochemical outcome. This can be deduced from the fact that all ligands share this group, but different senses of stereo induction were observed. Therefore, it seems that the primary source of enantiodiscrimination is the C−H···π attractive interaction between the $\eta^6$ ligand and the π-cloud of the approaching aromatic ketone, as proposed in section I.3.2.4. Still, a good ligand coordination leading to an undistorted complex geometry is the prerequisite for those interactions to be effective.

When comparing CIL **3** and **15**, it seems that the additional BOC group is greatly beneficial, leading to an enhanced enantioselectivity. As reported in the literature for the Tsdpen ligand, the oxygen lone pairs of $SO_2$ in the tosyl substituent are the sole reason for the high enantioselectivity compared to the corresponding amino alcohol ligands, lacking this group.[31] The same explanation presents itself in the case of CIL **15**, bearing a carbonyl oxygen at the same position in the ligand as the $SO_2$ group in the Tsdpen ligand. The interaction of the oxygen lone pairs and the π-cloud of the approaching aromatic ketone leads to a repulsion between those two, thereby destabilizing the less favored diastereomeric transition state. A higher energy difference between favored and disfavored diastereomeric transition state will consequently lead to a higher enantiomeric excess.

Moreover, it seems that the stereochemistry at the carbon atom next to the OH group (**3**, **6**) or the differently substituted amine functionalities in CIL **12**, **15** and **16** is determining the stereochemistry of

the product (see Table 3). Hence, a corresponding (*S*) configuration in the ligand will lead to the (*S*) enantiomer being the major one, while (*R*) configuration leads to the preferred formation of the (*R*) enantiomer. This assumption is nicely supported by the result obtained for the amino alcohol based ligands **3** and **6**. The inversion of the stereocenter next to the OH group from (*S*) in CIL **3** to (*R*) in CIL **6** as the sole modification in the molecule led subsequently also to the inversion of product stereochemistry. The inversion for CIL **12** due to dimethylation was already discussed above.

<u>Effects of ligand modifications on the transition state</u>

It seems that the NH functionality next to the cationic pyridinium head group is the one involved in the transition state. For CIL **3** and **12** this is obviously the only possibility to interact with the substrate via hydrogen bonding in the transition state.

In case of CIL **15** it can be assumed that the hydrogen atom at the amide nitrogen is far less acidic than the one at the secondary amine functionality. Therefore, proton transfer to the substrate would be more likely from the latter. Moreover, repulsive forces between the BOC group and the π-cloud of the aromatic ketone make the involvement of the amide nitrogen in the transition state far less likely. Consequently, the secondary amine functionality has to participate in the transition state.

For CIL **16**, the similarity with CIL **3** concerning the obtainable enantioselectivity would also suggest that the secondary amine is involved in the transition state. The lower activity compared with the corresponding amino alcohol can be attributed to the rate acceleration effect observed for the latter. In general, it has to be considered that the pyridinium head group is causing steric crowding around the NH group, making it less accessible for the ketone substrate. This will lead to a decrease in activity compared to a primary amine, as has already been reported in literature.[5]

Considering the different effects mentioned above, the following catalytic cycle employing CIL **15** as the chiral ligand can be proposed (Scheme 17). Herein, the NH functionality next to the pyridinium head group is participating in the catalytic cycle.
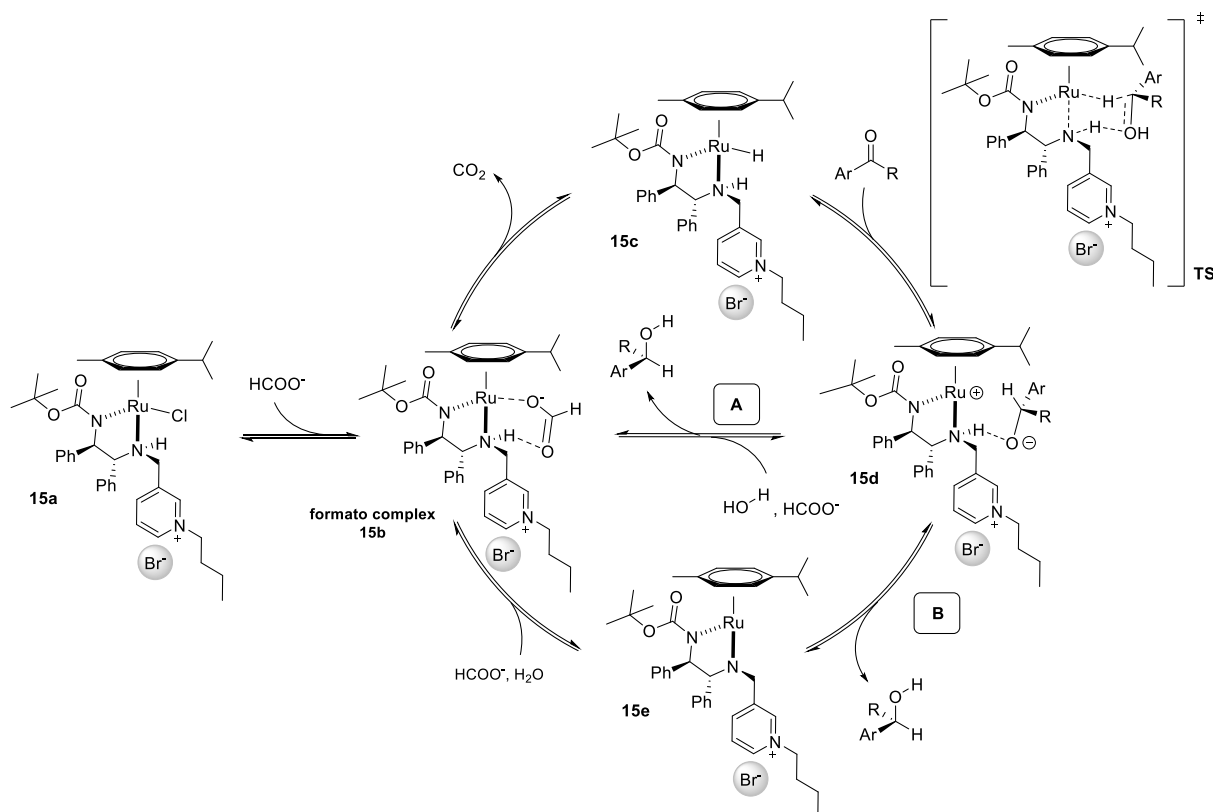


*Scheme 17. Proposed catalytic cycle employing CIL 15 as chiral ligand*

The precatalyst **15a** will form upon mixing the catalyst precursor [Ru(*p*-cymene)Cl$_2$]$_2$ and CIL **15** in water, whereby HCl is released. Upon addition of sodium formate, the formato complex **15b** can form, which will eliminate $CO_2$ to give the Ru-hydride complex **15c**. This active species can now reduce the ketone substrate via hydride transfer, forming an intimate ion pair **15d**. Subsequent proton transfer to the substrate can occur either from the ligand (route **B**) or from a water molecule (route **A**). To regenerate the secondary amine functionality in **15e**, a proton from a water molecule is abstracted. Hence, in either pathway a water molecule has to deliver a proton, leading to the formation of hydroxide ions, explaining the observed increase in pH in the course of the reaction. Subsequent interaction with another formate ion leads again to the formation of the formato complex **15b**, closing the catalytic cycle.

### III.2.1 Parameter Optimization

After CIL **15** was identified as the most promising ligand for aqueous ATH, the reaction parameters were further optimized for this ligand. Hereby, the reaction time and temperature were varied while keeping the other parameters, such as catalyst and substrate loading, constant. An overview of the obtained results is given in Table 4.

*Table 4. Optimization of reaction conditions for CIL 15*

| Entry[a] | T [°C] | Time [h] | % Conversion[c] | % ee[d] |
|:---:|:---:|:---:|:---:|:---:|
| 1 | 40 | 24 | >99 | 90 (*R*) |
| 2 | 40 | 6 | 95 | 90 (*R*) |
| 3 | 40 | 1 | 30 | >99 (*R*) |
| 4 | 25 | 24 | 92 | 91 (*R*) |
| 5 | 25 | 6 | 57 | 94 (*R*) |
| 6 | 60 | 1 | 97 | 90 (*R*) |
| 7[b] | 40 | 24 | >99 | 93 (*R*) |

[a] Performed with 2 mmol acetophenone, 10 mmol $HCO_2Na$, 0.5 mol% $[Ru(p\text{-}cymene)Cl_2]_2$ and 1.05 mol% CIL **15** in 4 mL $H_2O$. [b] Performed with 0.02 mmol RuCl[(R,R)-Tspden](p-cymene), 2 mmol acetophenone, 10 mmol $HCO_2Na$ in 4 mL $H_2O$ [c] Determined by HPLC analysis. [d] Determined by using a DAICEL Chiralcel IB column.

The results show that the developed hydrophilic ligand is indeed very active, even at temperatures as low as 25 °C, reaching almost full conversion within 24 h. This is remarkable, considering that most catalyst systems in ATH are rather sluggish in substrate conversion below 40 °C. Another interesting observation concerns the result obtained at 60 °C. Not only is the reaction completed within 1 h, but the catalyst with CIL **15** is also able to retain the excellent enantioselectivity, even at higher temperatures. This is rather unexpected, since a decrease in enantiomeric excess is usually observed for increasing reaction temperatures. For comparison, the reduction of acetophenone was also performed with the Noyori-Ikariya catalyst RuCl[(*R*,*R*)-Tspden](*p*-cymene) at 40 °C for 24 h (Entry 7). As can be seen, the catalyst is indeed very active, giving full conversion within 24 h. Concerning the enantioselectivity, the result clearly shows that CIL **15** can compete with the state of the art system, giving 90% ee compared to 93% ee for the Noyori-Ikariya catalyst under identical conditions (Entry 1 and 7). These results highlight the exceptional performance of the newly designed hydrophilic chiral ionic ligand **15**.

## III.2.2 Influence of Reaction Medium

To further demonstrate the beneficial effects of water as reaction medium on ATH, a comparative run was conducted in the standard reaction medium and donor isopropanol.

*Table 5. Comparison between $H_2O$ and isopropanol as reaction medium*

| Entry | Solvent | T [°C] | Time [h] | % Conversion[c] | % ee[d] |
|-------|---------|--------|----------|-----------------|---------|
| 1[a] | $H_2O$ | 40 | 24 | 100 | 90 |
| 2[b] | Isopropanol | 40 | 24 | 36 | 72 |

*[a] Performed with 2 mmol acetophenone, 10 mmol $HCO_2Na$, chiral ionic ligand 15 (0.02 mmol), [Ru(p-cymene)$Cl_2$]$_2$ (0.01 mmol) in 4 mL $H_2O$. [b]Performed with acetophenone (2 mmol, 0.1 M in isopropanol), KOH (0.04 mmol), chiral ionic ligand 15 (0.02 mmol), [Ru(p-cymene)$Cl_2$]$_2$ (0.01 mmol). [c] Determined by HPLC analysis. [d] Determined by HPLC analysis using a DAICEL Chiralcel IB column.*

The results in Table 5 clearly show that water is not only beneficial for the catalyst activity but also for the selectivity. This can be largely attributed to the ability of water to form hydrogen bonds, which can stabilize the transition state, lowering the activation barrier for the rate limiting hydride transfer. At the same time hydrogen bonding will also lock the substrate in its position, enhancing enantioselectivity. Since isopropanol is not able to form such a hydrogen bonding network, its possibilities to positively affect the transition state are limited, resulting in lower conversion and enantiomeric excess.

## III.2.3 Influence of Chain Length

Conducting asymmetric transfer hydrogenations in water consequently leads to a biphasic reaction mixture, as most organic substrates are not soluble in water. Hence, it can be expected that the efficient mixing of the two phases is a rate limiting factor. To facilitate substrate-catalyst interaction, the use of surfactants has been reported in literature.[18] As ionic liquids with an appropriate alkyl chain length can act as surfactants as well, it was a plausible idea to investigate this effect on the current reaction system. Therefore, the chain length at the pyridinium head group in CIL **15** was increased to $C_{12}$ in CIL **17**, to combine hydrophilic and surfactant like properties in the ligand. The effect of the different chain length on aqueous ATH of acetophenone was investigated at 40 °C with online infrared monitoring of substrate conversion at 955 cm$^{-1}$.
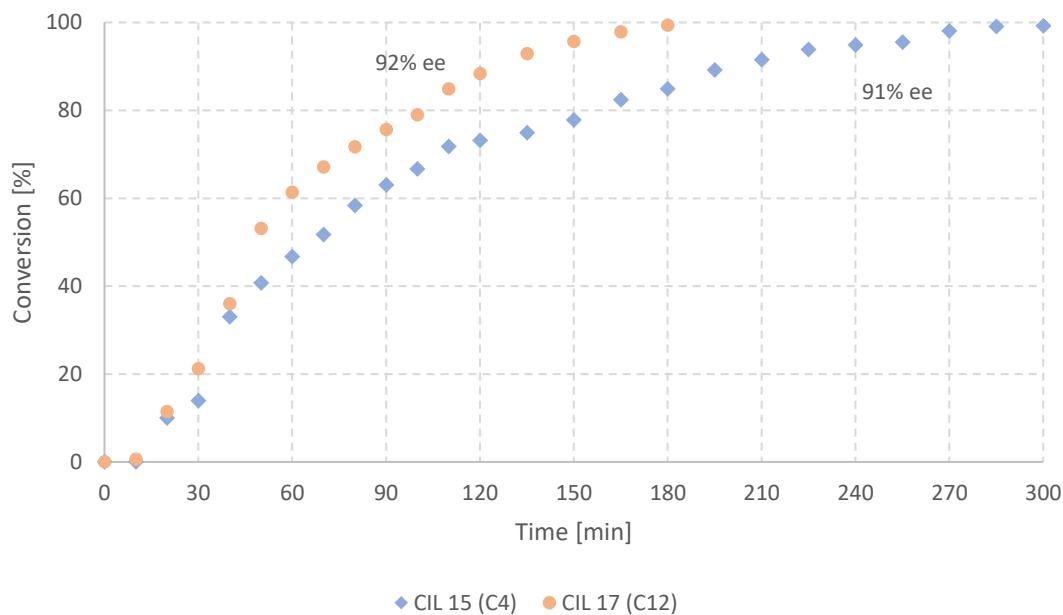
*Figure 24. Conversion of acetophenone monitored via IR*

*Performed with 2 mmol acetophenone, 10 mmol HCO$_2$Na, chiral ionic liquid (0.021 mmol) and [Ru(p-cymene)Cl$_2$]$_2$ (0.01 mmol) in 4 mL H$_2$O*

As can be seen from the chart above, the reaction is faster when CIL **17** with the longer C$_{12}$ alkyl chain is employed as the ligand. The reaction reaches full conversion after only 3 h, whereas the reaction using CIL **15** with the shorter C$_4$ alkyl chain takes about twice as long.

To investigate whether the formation of micelles plays a role in the rate enhancement with CIL **17**, dynamic light scattering (DLS) measurements were conducted.[2] Although the formation of micelles for ligands bearing a dodecyl chain has been reported in literature,[42,43] no evidence could be found for CIL **17**. In fact, the turbid appearance of the reaction medium suggested the formation of larger aggregates, and DLS results indicate that the ligand after coordination with the Ru precursor forms larger vesicles, with diameters of 64.52 ± 22.78 nm for CIL **15** and 118.2 ± 42.89 nm for CIL **17**. However, it seems that these larger vesicles are forced to form smaller aggregates upon addition of sodium formate. Not only was a clear solution obtained after salt addition, DLS also clearly showed the formation of small aggregates in a size range of 0.64 ± 0.08 nm for CIL **15** and 0.64 ± 0.07 nm for CIL **17**. The results are depicted in Figure 25 and Figure 26.

---

[2] DLS measurements were conducted under the supervision of Dipl.-Ing. Dr. Ronald Zirbs from the Department of Biologically inspired materials at the University of Natural Resources and Life Sciences, 1180 Vienna.
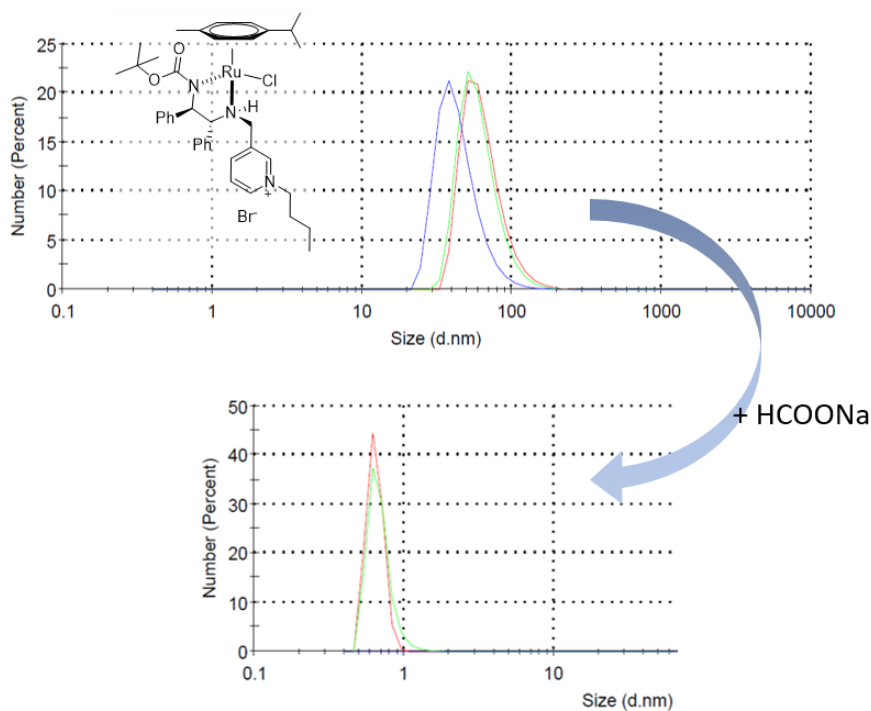
*Figure 25. DLS results for Ru-catalyst formed with CIL 15 before and after addition of sodium formate*
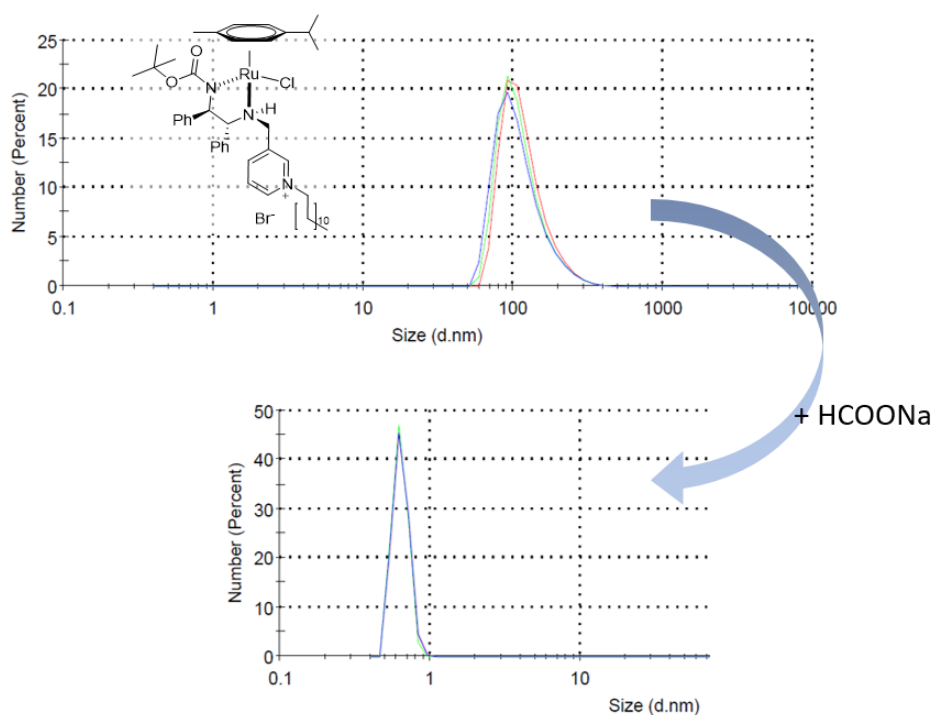


*Figure 26. DLS results for Ru-catalyst formed with CIL 17 before and after addition of sodium formate*

Based on these results, it is difficult to identify the supramolecular assembly of the chiral ionic ligand, and more investigations are clearly required. Although micelle formation does not seem as a likely explanation for the enhanced reaction rate, increasing the chain length to $C_{12}$ has nonetheless a positive effect. Moreover, the enantioselectivity seems unaffected from a change in chain length, as both ligands display similar selectivity with 91% ee and 92% ee, respectively.

## III.2.4      Substrate Scope

To investigate the substrate scope, different aromatic, prochiral ketones were chosen, featuring electron-withdrawing as well as electron-donating substituents. The reactions were performed at 25 °C for 24 h, as those conditions have previously been identified as ideal. To investigate the influence of ligand chain length, the substrates were reduced employing both CIL **15** and **17**. The obtained results are summarized in Table 6.

*Table 6. Investigation of substrate scope*

| Entry[a] | Substrate | CIL 15 (C$_4$) | | CIL 17 (C$_{12}$) | |
|---|---|---|---|---|---|
| | | Yield [%][b] | ee [%][c],[d] | Yield [%][b] | ee [%][c],[d] |
| **1** |  | 68 | 82 (*R*) | 54 | 85 (*R*) |
| **2** |  | 76 | 81 (*R*) | 58 | 85 (*R*) |
| **3** |  | 82 | 97 (*R*) | 62 | 98 (*R*) |
| **4** |  | 74 | 39 (*R*) | 54 | 86 (*R*) |
| **5** |  | 73 | 93 (*R*) | 44 | 96 (*R*) |
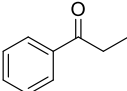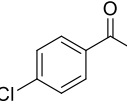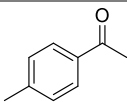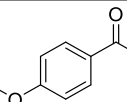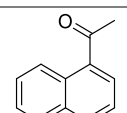
*[a] Performed with 2 mmol ketone, 10 mmol HCO$_2$Na, 0.5 mol% [Ru(p-cymene)Cl$_2$]$_2$ and 1.05 mol% chiral ionic ligand in 4 mL H$_2$O at 25 °C for 24 h. [b] Isolated yield after column chromatography. [c]Determined by HPLC using a DAICEL Chiralcel IB or AHS column. [d] Absolute configuration determined via optical rotation and comparison with literature values.*

For CIL **15**, all ketones performed well, affording the corresponding alcohols in 68% - 82% isolated yield. Apart from 4-methoxyacetophenone (entry 4), excellent selectivities >80% could be obtained. One plausible explanation for this deviation is that the oxygen lone pairs of the methoxy substituent are interfering with the enantiodiscriminating interactions in the transition state, overall lowering the enantioselectivity. Comparing those results with the ones obtained for CIL **17** it can be observed that the yields are generally lower when a longer alkyl chain is present in the ligand. This suggests that the accessibility of the active center for the ketone substrate is reduced due to steric crowding of the long alkyl chain. This seems contrary to what was observed during the kinetic experiments in III.2.3, where CIL **17** displayed higher activity. However, it has to be kept in mind that the reactions were carried out

under different temperatures (25 °C vs. 40 °C) and the experimental setup was different, which might explain those otherwise contradicting results. Nonetheless, as could already be observed, a longer alkyl chain seems to have no effect or even a positive effect on enantiodiscrimination, as the obtained ee values are in the range of the ones obtainable with CIL **15** or slightly higher. Especially the result for 4-methoxyacetophenone (entry 4) is interesting, as the enantiomeric excess could be doubled employing CIL **17**, reaching an ee value of 86% compared to 39%. This suggests that a longer alkyl chain might be beneficial for substrates being difficult to reduce otherwise with a high enantiomeric excess, although at the cost of reactivity.

## III.2.5    Catalyst Recycling

The employed catalysts in asymmetric transfer hydrogenation feature precious transition metals (Ru, Rh, or Ir) and the ligands are often costly in their synthesis. Therefore, efficient catalyst recycling is a critical point.

The synthesized ligands CIL **3**, **12**, **15** and **16** all have an ionic pyridinium head group, which should facilitate catalyst recycling by immobilizing the catalyst in the aqueous phase, whilst the product can be extracted with a solvent. For this purpose, CIL **15** was employed in the test reaction and two recycling strategies were tested:

(1) classical solvent extraction of the product with *n*-hexane or Et$_2$O and

(2) extraction with supercritical CO$_2$ (scCO$_2$)

Subsequently, a fresh batch of the substrate acetophenone and the hydrogen donor sodium formate were added and the reaction run again, as depicted in Figure 27.
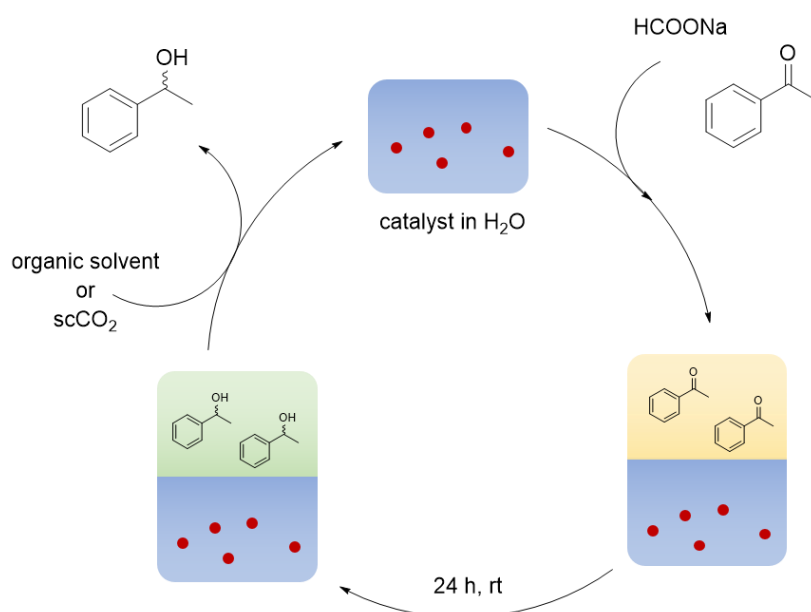


*Figure 27. Schematic catalyst recycling strategy*

Using classical organic solvents for product extraction and catalyst recycling offers the advantage that no special equipment is necessary. For first experiments, $Et_2O$ was used as extracting solvent, which was purged with argon prior to use. However, on addition of the organic solvent to the reaction mixture, the latter turned black immediately, suggesting that the catalyst was decomposing. Hence, *n*-hexane was chosen as alternative extracting solvent. It was purged with argon prior to use as well and the product could be extracted with approximately 90%. Moreover, no color changes in the aqueous phase could be observed. After extraction, the aqueous phase was subjected to reduced pressure for a short time to remove remaining *n*-hexane. Subsequently, a fresh batch of sodium formate and acetophenone were added and the reaction run again under the stated conditions. However, almost no conversion could be observed for the second run (Table 7), suggesting that the recycling protocol suffers from probable catalyst leaching and either catalyst decomposition or inhibition.

*Table 7. Results for catalyst recycling with n-hexane and scCO₂*

| Entry | extracting solvent | run | conversion[c] [%] | ee[d] [%] |
|:---:|:---:|:---:|:---:|:---:|
| 1 | *n*-hexane[a] | 1st | 97 | 90 |
| 2 | | 2nd | 4 | >99 |
| 3 | scCO$_2$[b] | 1st | 93 | 89 |
| 4 | | 2nd | 2 | >99 |

*[a] Performed with 2 mmol ketone, 10 mmol HCO₂Na, 0.5 mol% [Ru(p-cymene)Cl₂]₂ and 1.05 mol% CIL **15** in 4 mL H₂O at 25 °C for 24 h. n-hexane was purged with argon prior to use. Extraction was performed with 3 x 3 mL n-hexane. [b] ᵃ Performed with 2 mmol ketone, 10 mmol HCO₂Na, 0.5 mol% [Ru(p-cymene)Cl₂]₂ and 1.05 mol% CIL **15** in 4 mL H₂O at 25 °C for 20 h. Extractions were performed at 40 °C with a flowrate of 5 mL/min at a pressure of 13 MPa for 30 min. [c] Determined by HPLC analysis. [d] Determined by HPLC analysis using a DAICEL Chiralcel IB column.*

The second recycling strategy involves product extraction with supercritical carbon dioxide (scCO$_2$). Using scCO$_2$ for extraction and recycling offers some advantages over classical solvents. It is non-toxic, non-flammable and can be removed from the product by simple pressure release after the extraction, as $CO_2$ will evaporate. Especially using ionic ligands takes advantage of the fact that the solubility for ionic species is extremely low in scCO$_2$. However, special equipment for the use of scCO$_2$ is needed, including a pressurized reactor. A schematic setup for the continuous extraction of the reaction mixture with scCO$_2$ is depicted in Figure 28.
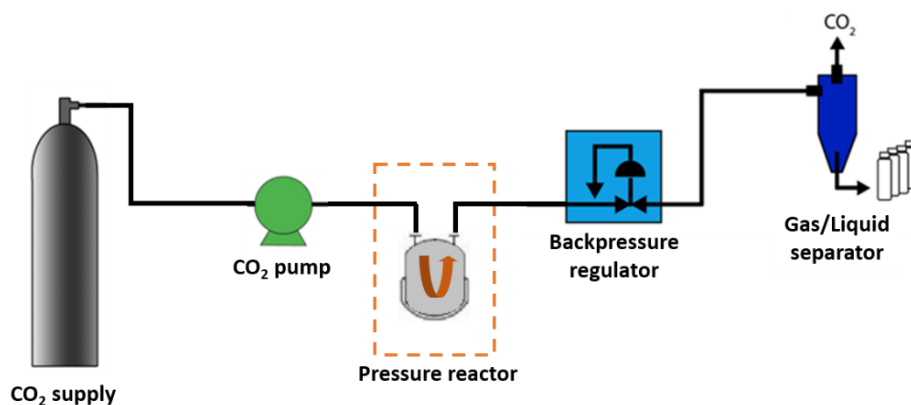
*Figure 28. Schematic setup for extraction with scCO$_2$*

The catalyst recycling with scCO$_2$ was carried out as follows: The reaction was run in a Schlenk tube and after the stated time the reaction mixture was transferred into the pressure reactor. In this step, slight product losses could not be avoided. The extraction was carried out at 40 °C for 30 min and was almost quantitatively. Subsequently, the aqueous phase was again transferred into a Schlenk tube, and no color changes could be detected. As it has already been observed in literature that CO$_2$ can have an inhibiting effect on the catalyst,[45] the aqueous solution was again purged with argon for 15 min. Subsequently, a fresh batch of sodium formate and acetophenone were added and the reaction run again. However, as was already the case for conventional solvent extraction, again no conversion could be observed in the second run. To ensure that changes in pH are not responsible, the pH was checked in a second experiment. After extraction, the aqueous solution displayed a rather neutral pH and after addition of sodium formate turned again slightly basic. Nonetheless, no conversion could be observed in the second run. Hence, either problems with maintaining an inert atmosphere or catalyst leaching or decomposition are again possible explanations for the loss of activity.

# IV Conclusion

In the present work, the efficient synthesis of chiral ionic ligands from enantiopure starting materials was demonstrated. In case of amino alcohol based chiral ligands **3** and **6**, the synthesis was performed in a straightforward two step procedure. Alkylation of the pyridine head group was selective and gave the final chiral ionic ligands in high overall yield.

In case of diamine based chiral ligands the use of protecting groups for the selective modification of the amine functional groups was necessary. Thereby, the importance of the proper choice of substituent on the amine functionalities was further demonstrated. By choosing an electron withdrawing BOC group as substituent for the chiral ligand **15**, a highly active and selective catalyst could be obtained in only three synthesis steps.
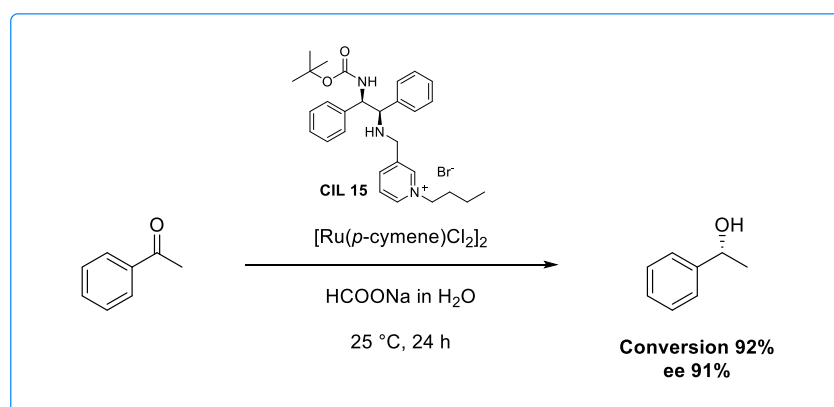


*Scheme 18. Asymmetric transfer hydrogenation of acetophenone with best performing ligand **15** under optimized conditions*

The obtained hydrophilic chiral ionic ligands were successfully applied in the Ru-catalyzed asymmetric transfer hydrogenation of acetophenone in water. The chiral ionic ligands provided variable enantioselectivities and yields. The BOC-substituted chiral ionic ligand **15** showed excellent performance even at room temperature, and is able to compete with the current benchmark ligand systems for asymmetric transfer hydrogenations. When the scope was expanded to different aromatic ketones, high selectivities and yields could again be observed, demonstrating the versatility of the developed ligand. As catalyst recycling is a critical issue for transition metal catalyzed reactions, two different recycling strategies were employed. However, both protocols seemed to suffer from catalyst leaching and deactivation, and need further improvement.

# V  Experimental Part

## V.1  Material and Methods

All reagents were purchased from commercial suppliers and used without further purification unless noted otherwise. Dichloromethane, methanol and toluene intended for anhydrous reactions were pre-distilled and desiccated on $Al_2O_3$ columns (PURESOLV, Innovative Technology).

Chromatography solvents were distilled prior to use. Column chromatography was performed on standard manual glass columns using silica gel from Merck (40-63 µm) with the eluates stated.

Preparative HPLC was performed on a Reveleris® Prep Purification System using a Maisch ReproSil 100 C18 column (250 mm x 4.6 mm ID, 5 µm) and $H_2O$/acetonitrile as eluent at a flowrate of 15 mL/min.

TLC-analysis was carried out using precoated aluminum-backed plates purchased from Merck (silica gel 60 F254). UV active compounds were detected at 254 nm.

$^1H$ and $^{13}C$ NMR spectra were recorded from $CDCl_3$, MeOD or $D_2O$ solutions on a Bruker AC 200 (200 MHz) or Bruker Advance UltraShield 400 (400 MHz) spectrometer and chemical shifts (δ) are reported in ppm using tetramethylsilane as internal standard. Coupling constants (J) are reported in Hertz (Hz). The following abbreviations were used to explain the multiplicities: s = singlet, d = doublet, t = triplet, q = quartet, m = multiplet, brs = broad singlet.

Enantiomeric composition was determined *via* HPLC on a DAIONEX UPLC, equipped with a PDA plus detector (190-360 nm) using DAICEL IB or AS-H columns (250 x 4.60 mm) as stationary phase. The following methods were used to separate the enantiomers:

> (A) *n*-hexane/*i*-PrOH 98.5:1.5, flowrate 1 mL/min, column IB
>
> (B) *n*-heptane/*i*-PrOH 93:7, flowrate 1 mL/min, column IB
>
> (C) *n*-heptane/*i*-PrOH 98:2, flowrate 0.7 mL/min, column AS-H

Absolut configuration was determined by measurement of optical rotation values and comparison with literature data. Optical rotation was measured on an Anton Paar MCP500 polarimeter at the specified conditions. The concentrations are stated in g/ 100 mL.

Melting points above room temperature were measured on an automated melting point system OPTI MELT of Stanford ResearchSystems and are uncorrected.

Infrared spectra were recorded on a Perkin-Elmer Spectrum 65 FT IR spectrometer equipped with a specac MK II Golden Gate Single Reflection ATR unit. Online FT IR measurements were conducted with a Mettler Toledo ReactIR 15 equipped with a diamond sensor and a MCT detector.

HR-MS analysis was carried out from methanol solutions (*c* 10 ppm) by using an HTC PAL system auto sampler (CTC Analytics AG), an Agilent 1100/1200 HPLC with binary pumps, degasser and column thermostat (Agilent Technologies) and Agilent 6230 AJS ESI–TOF mass spectrometer.

## V.2    Amino Alcohol derived Chiral Ionic Ligands

The preparation for amino alcohol based chiral ionic ligands **3** and **6** and the corresponding precursors **2** and **5** was adapted from literature.[43]

### V.2.1    (1*S*,2*R*)-1,2-Diphenyl-2-[(pyridin-3-ylmethyl)amino]ethanol 2



$C_{20}H_{20}N_2O$
304.39
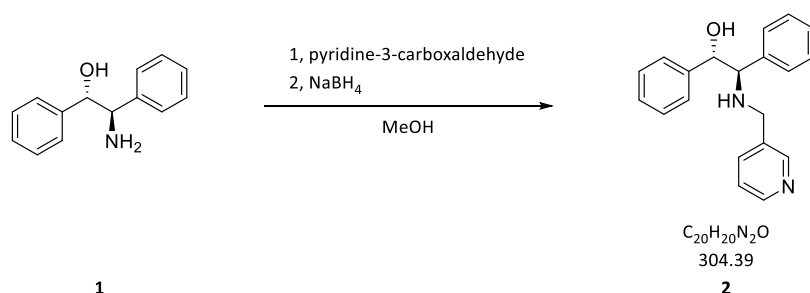
(1*S*,2*R*)-2-Amino-1,2-diphenylethanol **1** (1.0 equiv., 9.38 mmol, 2.00 g) was dissolved in 100 mL of anhydrous MeOH. Activated molecular sieve 4 Å (5.00 g) and freshly distilled pyridine-3-carboxaldehyde (1.0 equiv., 9.38 mmol, 0.88 mL) were added and the reaction mixture refluxed overnight. After TLC indicated complete conversion NaBH$_4$ (1.5 equiv., 14 mmol, 0.53 g) was added in small portions and the mixture was stirred at room temperature until complete conversion. The reaction mixture was filtered over Celite and hydrolyzed with H$_2$O. MeOH was removed under reduced pressure. The aqueous phase was extracted with CH$_2$Cl$_2$, dried over Na$_2$SO$_4$ and the solvent removed under reduced pressure. The crude product was crystallized from toluene to yield **2** as colorless crystals (2.31 g, 81%).

**¹H NMR** (400 MHz, CDCl₃)        δ = 8.37 (dd, J$_1$ = 1.54 Hz, J$_2$ = 4.92 Hz, 1H), 8.27 (d, J = 1.84 Hz, 1H), 7.41 − 7.37 (m, 1H), 7.27 − 7.24 (m, 1H), 7.21 − 7.05 (m, 10H), 4.73 (d, J = 6.14 Hz, 1H), 3.80 (d, J = 6.14 Hz, 1H), 3.60 (d, J = 13.82 Hz, 1H), 3.43 (d, J = 13.82 Hz, 1H), 2.87 (brs, 1H), 1.92 (brs, 1H).

Analytical data was in accordance with the literature.[43]

### V.2.2 1-Butyl-3-(((((1*S*,2*R*)-2-hydroxy-1,2-diphenylethyl)amino)methyl)pyridin-1-ium bromide 3
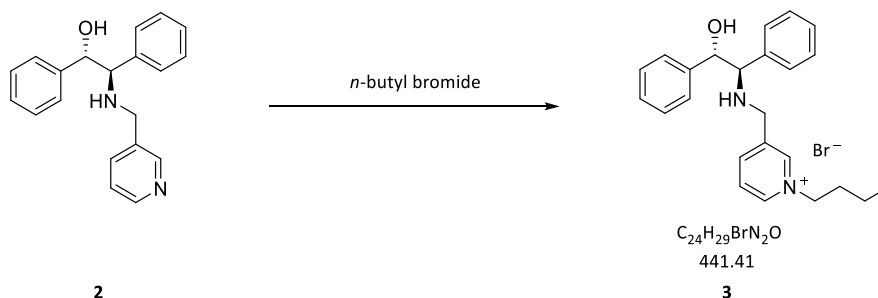


Compound **2** (1.0 equiv., 6.5 mmol, 2.00 g) and *n*-butyl bromide (1.2 equiv., 7.8 mmol, 0.84 mL) were mixed in a round bottom flask, sealed and heated to 80 °C for 17 h. Excess *n*-butyl bromide was evaporated to yield **3** as an orange solid (2.55 g, 88%), which was used without further purification.

**¹H NMR** (200 MHz, D₂O)  δ = 8.84 (d, J = 6.32 Hz, 1H), 8.69 (s, 1H), 8.49 (d, J = 8.55 Hz, 1H), 8.08 − 7.96 (m, 1H), 7.47 − 7.06 (m, 10H), 5.42 (d, J = 4.68 Hz, 1H), 4.62 (d, J = 4.68 Hz, 1H), 4.57 − 4.35 (m, 4H), 1.99 − 1.81 (m, 2H), 1.42 − 1.20 (m, 2H), 0.91 (t, J = 7.44 Hz, 3H).

Analytical data was in accordance with the literature.[43]

### V.2.3    (1*R*,2*R*)-1,2-Diphenyl-2-[(pyridin-3-ylmethyl)amino]ethanol 5
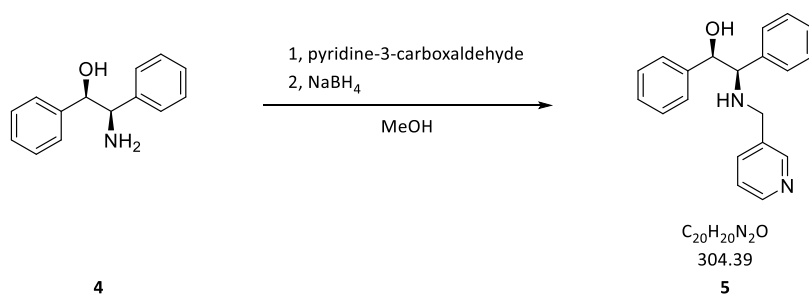


Compound **5** was prepared according to V.2.1 using (1*R*,2*R*)-2-amino-1,2-diphenylethanol **4** (1.0 equiv., 0.7 mmol, 150 mg), freshly distilled pyridine-3-carboxaldehyde (1.0 equiv., 0.7 mmol, 66 µL) and activated molecular sieve 4 Å (100 mg) in 10 mL anhydrous MeOH. After complete reaction of amino alcohol **4**, NaBH$_4$ (1.2 equiv., 0.8 mmol, 32 mg) was added. Product **5** could be obtained as colorless solid after crystallization from toluene (183 mg, 85%).

| | |
|---|---|
| **Melting Point** | 109-111 °C |
| **$^1$H NMR** (400 MHz, CDCl$_3$) | δ = 8.36 (d, J = 2.19 Hz, 1H, *H*-pyridine), 8.34 (s, 1H, *H*-pyridine), 7.52 (d, J = 3.83 Hz, 1H, *H*-pyridine), 7.17 − 6.93 (m, 11H, *H*-pyridine, *H*-arom), 4.54 (d, J = 4.24 Hz, 1H, C*H*-OH), 4.25 (brs, 1H, O*H*), 3.66 − 3.57 (m, 2H, C*H*-NH, NH-C*H$_2$*), 3.48 (d, J = 6.74 Hz, 1H, NH-C*H$_2$*), 2.23 (brs, 1H, N*H*). |
| **$^{13}$C NMR** (100 MHz, CDCl$_3$) | δ = 149.7 (d, *C*-pyridine), 148.6 (d, *C*-pyridine), 141.1 (s, *C*-arom), 139.4 (s, *C*-arom), 136.0 (d, *C*-pyridine), 135.3 (s, *C*-pyridine), 128.4 (d, *C*-arom), 128.0 (d, *C*-arom), 127.7 (d, *C*-arom), 127.6 (d, *C*-arom), 126.8 (d, *C*-arom), 123.5 (d, *C*-pyridine), 78.0 (d, *C*H-OH), 69.7 (d, *C*H-NH), 48.7 (t, NH-*C*H$_2$). |
| **HRMS** (ESI-TOF) | m/z: [M + H]$^+$ Calculated for C$_{20}$H$_{20}$N$_2$O 305.1648; Found 305.1647 |
| **Specific rotation** | α$_D^{20}$ = +7.3 (*c* 1.05, MeOH) |
| **v$_{max}$/cm$^{-1}$** | 3202 (O−H), 1579 (C=C), 1452 (C−H), 759 (C−H arom), 699 (C−H arom) |

### V.2.4      1-Butyl-3-((((1*R*,2*R*)-2-hydroxy-1,2-diphenylethyl)amino)methyl)pyridin-1-ium bromide 6
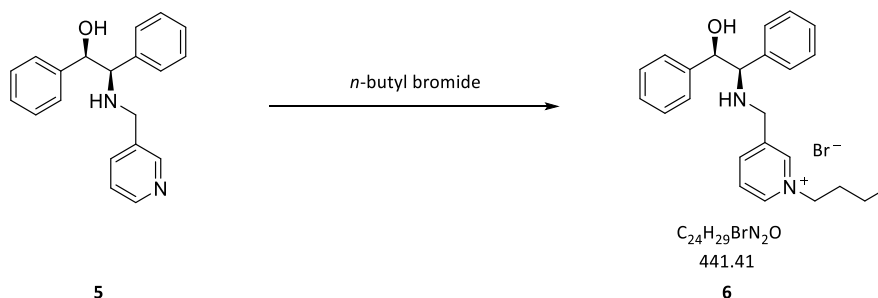


Compound **6** was prepared according to V.2.2 by reacting compound **5** (1.0 equiv., 0.3 mmol, 105 mg) and *n*-butyl bromide (1.2 equiv., 0.4 mmol, 44 µL) at 80 °C until $^1$H NMR indicated complete conversion. The product was obtained as orange foam (150 mg, 98%) and used without further purification.

| | |
|---|---|
| **$^1$H NMR** (400 MHz, MeOD) | δ = 8.87 (s, 1H, *H*-pyridine), 8.83 (d, J = 6.42 Hz, 1H, *H*-pyridine), 8.43 (d, J = 7.70 Hz, 1H, *H*-pyridine), 7.99 – 7.94 (m, 1H, *H*-pyridine), 7.20 – 7.08 (m, 10H, *H*-arom), 4.76 (d, J = 8.59 Hz, 1H, C*H*-OH), 4.56 (t, J = 7.64 Hz, 2H, N-C*H₂*), 4.01 (d, J = 15.27 Hz, 1H, NH-C*H₂*), 3.91 (d, J = 15.27 Hz, 1H, NH-C*H₂*), 3.86 (d, J = 8.59 Hz, 1H, C*H*-NH), 2.02 – 1.93 (m, 2H, N-CH₂-C*H₂*), 1.48 – 1.37 (m, 2H, N-(CH₂)₂-C*H₂*), 1.04 (t, J = 7.32 Hz, 3H, N-(CH₂)₃-C*H₃*). |
| **$^{13}$C NMR** (100 MHz, MeOD) | δ = 146.2 (d, *C*-pyridine), 145.2 (d, *C*-pyridine), 144.0 (d, *C*-pyridine), 143.2 (s, *C*-pyridine), 143.0 (s, *C*-arom), 139.9 (s, *C*-arom), 129.8 (d, *C*-arom), 129.2 (d, *C*-arom), 128.7 (d, *C*-arom), 128.6 (d, *C*-arom), 128.4 (d, *C*-arom), 128.2 (d, *C*-pyridine), 78.9 (d, *C*H-OH), 71.1 (d, *C*H-NH), 62.7 (t, N-*C*H₂), 48.6 (t, NH-*C*H₂), 34.3 (t, N-CH₂-*C*H₂), 20.3 (t, N-(CH₂)₂-*C*H₂), 13.8 (q, N-(CH₂)₃-*C*H₃). |
| **HRMS** (ESI-TOF) | m/z: [M]⁺ Calculated for C₂₄H₂₉N₂O 361.2274; Found 361.2278 |
| **Specific Rotation** | α_D²⁰ = +33.4 (*c* 0.95, MeOH) |
| **v_max/cm⁻¹** | 3306 (O−H), 2960 (C−H), 1498 (C=C), 1453 (C−H δ_a), 1377 (C−H δ_a), 757 (C−H arom), 703 (C−H arom) |

## V.3    Diamine derived Chiral Ionic Ligands

### V.3.1        2-[(1*R*,2*R*)-2-Amino-1,2-diphenylethyl]- 1*H*-isoindole-1,3(2*H*)-dione 8



$C_{22}H_{18}N_2O_2$
342.40

**7**                                                        **8**
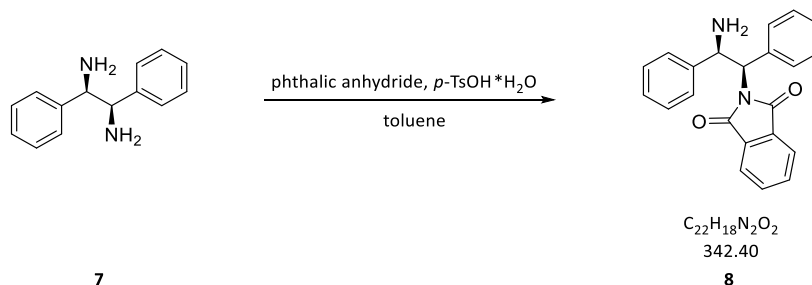
Compound **8** was prepared according to the literature procedure.[46]

In a round bottom flask *p*-TsOH· $H_2O$ (1.0 equiv., 4.7 mmol, 0.89 g) was dissolved in anhydrous toluene. Activated molecular sieve 4 Å (3.00 g), phthalic anhydride (1.1 equiv., 5.2 mmol, 0.76 g) and (1*R*,2*R*)-1,2-diphenyl-1,2-ethanediamine (1.0 equiv., 4.7 mmol, 1.0 g) were added and the reaction mixture was refluxed overnight. The mixture was filtered over Celite, washed with $CH_2Cl_2$ and stirred with saturated $Na_2CO_3$ solution. The phases were separated and the organic phase was dried over $Na_2SO_4$. The solvent was removed under reduced pressure to yield **11** as pale yellow solid (1.25 g, 73%), which was used without further purification.

**¹H NMR** (400 MHz, CDCl₃)      δ = 8.05 – 8.01 (m, 1H), 7.89 – 7.86 (m, 1H), 7.72 – 7.67 (m, 2H), 7.40 – 7.29 (m, 7H), 7.28– 7.22 (m, 3H), 5.61 (d, J = 5.63 Hz, 1H), 5.06 (d, J = 5.63 Hz, 1H).

**¹³C NMR** (100 MHz, CDCl₃)     δ = 162.4 (s), 160.5 (s), 140.6 (s), 138.8 (s), 138.1 (s), 132.8 (d), 129.2 (s), 129.2 (d), 129.0 (d), 128.3 (d), 128.2 (d), 126.6 (d), 126.0 (d), 124.1 (d), 123.3 (d), 88.8 (d), 65.5 (d).

Analytical data was in accordance with literature.[46]

## V.3.2  2-[(1*R*,2*R*)-2-(Dimethylamino)-1,2-diphenylethyl]-1*H*-isoindole-1,3(2*H*)-dione 9



C$_{24}$H$_{22}$N$_2$O$_2$
370.45
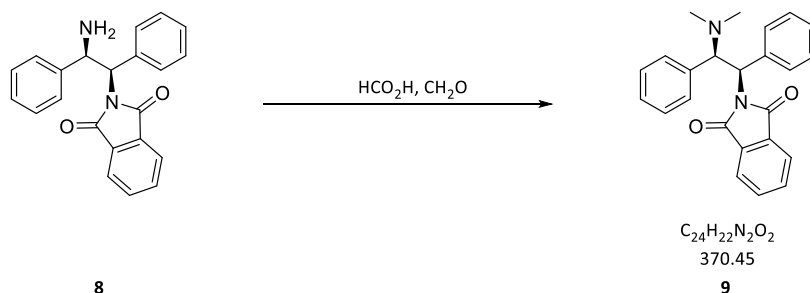
Procedure adapted from literature.[47]

Compound **8** (1.0 equiv., 2.9 mmol, 0.99 g) was dissolved in concentrated formic acid (98%, 14 mL) and stirred for 30 minutes. Formaldehyde (37% in H$_2$O, 12 mL) was added and the mixture refluxed until TLC indicated complete conversion. Remaining formaldehyde was removed under reduced pressure and the reaction mixture was neutralized with 4 M NaOH. After extraction with CH$_2$Cl$_2$ and drying over Na$_2$SO$_4$ the solvent was removed under reduced pressure to yield **9** as yellow solid (1.01 g, 94%).

**$^1$H NMR** (200 MHz, CDCl$_3$)     δ = 7.80 – 7.69 (m, 2H), 7.65 – 7.54 (m, 2H), 7.49 – 7.40 (m, 2H), 7.23 – 6.93 (m, 8H), 5.90 (d, J = 12.46 Hz, 1H), 5.14 (d, J = 12.46 Hz, 1H), 2.01 (s, 6H).

**$^{13}$C NMR** (100 MHz, CDCl$_3$)     δ = 168.6 (s), 137.5 (s), 133.7 (d), 132.6 (s), 129.6 (d), 128.3 (d), 127.7 (d), 127.6 (d), 127.2 (d), 123.1 (d), 65.9 (d), 54.8 (d), 40.8 (q).

Analytical data was in accordance with literature.[48]

### V.3.3 (1*R*,2*R*)-*N*¹,*N*¹-Dimethyl-1,2-diphenyl-1,2-ethanediamine 10
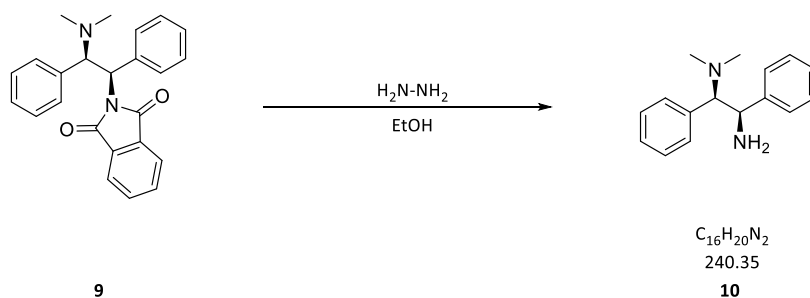


Procedure adapted from literature.[46]

Hydrazine hydrate (10 equiv., 11.6 mmol, 0.72 mL 50% solution in $H_2O$) was added to a dispersion of **9** (1.0 equiv., 1.2 mmol, 430 mg) in 15 mL EtOH and the reaction mixture was refluxed for 2 hours. After cooling to room temperature, the mixture was diluted with $Et_2O$ and the formed precipitate was removed via filtration. The organic phase was dried over $Na_2SO_4$ and the solvent removed under reduced pressure to yield **10** as yellow, viscous liquid (266 mg, 96%).

**¹H NMR** (400 MHz, CDCl₃)     δ = 7.15 − 7.10 (m, 2H), 7.07 − 6.95 (m, 5H), 6.94 − 6.86 (m, 3H), 4.34 (d, J = 10.50 Hz, 1H), 3.54 (d, J = 10.50 Hz, 1H), 2.19 (brs, 2H), 2.10 (s, 6H).

**¹³C NMR** (100 MHz, CDCl₃)     δ = 143.2 (s), 133.8 (s), 129.8 (d), 128.1 (d), 128.0 (d), 127.3 (d), 126.9 (d), 126.8 (d), 75.2 (d), 55.6 (d), 40.9 (q).

Analytical data was in accordance with literature.[49]

## V.3.4 (1*R*,2*R*)-*N*¹,*N*¹-Dimethyl-1,2-diphenyl-*N*²-(pyridin-3-ylmethyl)ethane-1,2-diamine 11



$C_{22}H_{25}N_3$
331.46

**10**                                   **11**
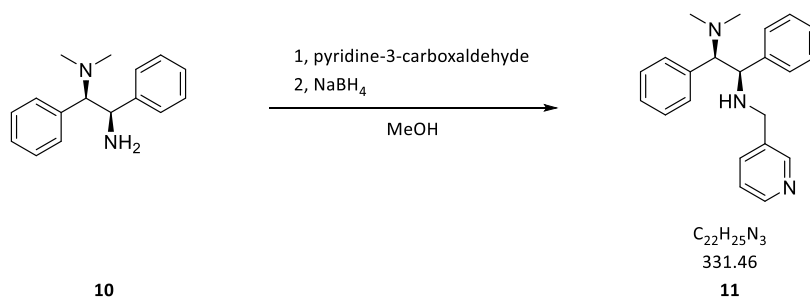
Compound **11** was prepared according to V.2.1 using compound **10** (1.0 equiv., 2.2 mmol, 535 mg) in 50 mL anhydrous MeOH, molecular sieve 4 Å (2.0 g) and freshly distilled pyridine-3-carboxaldehyde (1.0 equiv., 2.2 mmol, 0.2 mL) followed by the addition of NaBH$_4$ (1.5 equiv., 3.3 mmol, 126 mg) in small portions at room temperature. After purification via chromatography (45 g silica, CH$_2$Cl$_2$ : MeOH 40:1 + NEt$_3$) product **11** could be obtained as yellow solid (648 mg, 88%).

| | |
|---|---|
| **Melting Point** | 85-88 °C |
| **¹H NMR** (400 MHz, CDCl$_3$) | δ = 8.44 (d, J = 1.98, 1H, *H*-pyridine), 8.42 (dd, J$_1$ = 1.61 Hz, J$_2$ = 4.65 Hz, 1H, *H*-pyridine), 7.56 − 7.52 (m, 1H, *H*-pyridine), 7.18 − 7.13 (m, 3H, *H*-pyridine, *H*-arom), 7.08 − 6.93 (m, 6H, *H*-arom), 6.88 − 6.84 (m, 2H, *H*-arom), 3.96 (d, J = 10.74 Hz, 1H, C*H*-N(CH$_3$)$_2$), 3.67 − 3.60 (m, 2H, C*H*-NH, NH-C*H*$_2$), 3.46 (d, J = 13.64 Hz, 1H, NH-C*H*$_2$), 3.28 (brs, 1H, N*H*), 2.01 (s, 6H, N-(C*H*$_3$)$_2$). |
| **¹³C NMR** (100 MHz, CDCl$_3$) | δ = 149.9 (d, *C*-pyridine), 148.3 (d, *C*-pyridine), 141.1 (s, *C*-arom), 136.2 (s, *C*-arom), 136.0 (d, *C*-pyridine), 132.9 (s, *C*-pyridine), 129.9 (d, *C*-arom), 128.9 (d, *C*-arom), 127.9 (d, *C*-arom), 127.3 (d, *C*-arom), 127.0 (d, *C*-arom), 126.9 (d, *C*-arom), 123.3 (d, *C*-pyridine), 74.3 (d, C*H*-N(CH$_3$)$_2$), 61.6 (d, *C*H-NH), 48.5 (t, NH-*C*H$_2$), 40.6 (q, N-(*C*H$_3$)$_2$). |
| **HRMS** (ESI-TOF) | m/z: [M + H]$^+$ Calculated for C$_{22}$H$_{25}$N$_3$ 332.2121; Found 332.2129 |
| **Specific Rotation** | α$_D^{20}$ = −12.4 (*c* 1.05, MeOH) |
| **ν$_{max}$/cm$^{-1}$** | 3386 (N−H), 2935 (C−H), 1574 (C=C), 1451 (C−H), 696 (C−H arom) |

### V.3.5    1-Butyl-3-((((1*R*,2*R*)-2-(dimethylamino)-1,2-diphenylethyl)amino)methyl) pyridin-1-ium bromide 12



**11**                    **12**
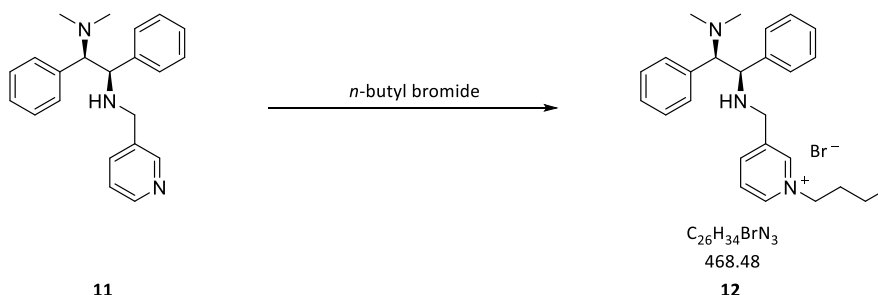
Compound **11** (1.0 equiv., 0.9 mmol, 300 mg) was mixed with *n*-butyl bromide (1.2 equiv., 1.1 mmol, 0.11 mL), sealed and heated to 60 °C. After 16 h excess *n*-butyl bromide was removed under reduced pressure to yield **12** as orange foam (373 mg, 87%), which was used without further purification.

For analytical purpose the product was purified via preparative HPLC.

**$^1$H NMR** (400 MHz, CDCl$_3$)    δ = 9.66 (s, 1H, *H*-pyridine), 8.84 (d, J = 5.60 Hz, 1H, *H*-pyridine), 8.35 (d, J = 7.83 Hz, 1H, *H*-pyridine), 7.95 – 7.85 (m, 1H, *H*-pyridine), 7.48 (m, 4H, *H*-arom), 7.25 – 7.16 (m, 3H, *H*-arom), 7.10 – 6.95 (m, 3H, *H*-arom), 5.09 (d, J = 11.64 Hz, 1H, C*H*-NH), 4.99 (d, J = 11.64 Hz, 1H, C*H*-N(CH$_3$)$_2$), 4.78 (t, J = 7.16 Hz, 2H, N-C*H*$_2$), 4.26 (d, J = 15.44 Hz, 1H, NH-C*H*$_2$), 3.88 (d, J = 15.44 Hz, 1H, NH-C*H*$_2$), 2.90 (s, 6H, N-(C*H*$_3$)$_2$), 2.05 – 1.96 (m, 2H, N-CH$_2$-C*H*$_2$), 1.41 – 1.28 (m, 2H, N-(CH$_2$)$_2$-C*H*$_2$), 0.89 (t, J = 7.21 Hz, 3H, N-(CH$_2$)$_3$-C*H*$_3$)

**$^{13}$C NMR** (100 MHz, CDCl$_3$)    δ = 144.7 (d, *C*-pyridine), 144.4 (d, *C*-pyridine), 142.3 (d, *C*-pyridine), 141.7 (s, *C*-arom), 138.0 (s, *C*-arom), 131.7 (d, *C*-pyridine), 130.2 (d, *C*-arom), 128.9 (d, *C*-arom), 128.7 (d, *C*-arom), 128.3 (d, *C*-arom), 127.9 (d, *C*-arom), 127.5 (d, *C*-arom), 127.5 (s, *C*-pyridine), 72.7 (d, *C*H-NH), 61.6 (t, N-*C*H$_2$), 60.8 (d, *C*H-N(CH$_3$)$_2$), 47.7 (t, NH-*C*H$_2$), 33.5 (t, N-CH$_2$-*C*H$_2$), 19.4 (t, N-(CH$_2$)$_2$-*C*H$_2$), 13.6 (q, N-(CH$_2$)$_3$-*C*H$_3$)

**HRMS** (ESI-TOF)    m/z: [M]$^+$ Calculated for C$_{26}$H$_{34}$N$_3$ 388.2747; Found 388.2750

**Specific Rotation**    α$_D$$^{20}$ = +24.9 (*c* 0.95, MeOH)

**v$_{max}$/cm$^{-1}$**    3406 (N−H), 2943 (C−H), 1498 (C=C), 1453 (C−H δ$_a$), 1377 (C−H δ$_a$), 757 (C−H arom), 703 (C−H arom)

### V.3.6 *N*-[(1*R*,2*R*)-2-Amino-1,2-diphenylethyl]-carbamic acid, 1,1-dimethylethyl ester 13



Compound **13** was prepared following the literature procedure.[44]

(1*R*,2*R*)-1,2-Diphenyl-1,2-ethanediamine (1.0 equiv., 7.0 mmol, 1.5 g) were dissolved in 10 mL anhydrous MeOH and cooled via ice bath. A 1 M solution of HCl in MeOH (1.2 equiv., 8.5 mmol, 8.3 mL) was slowly added and the mixture was subsequently stirred at r.t. for 15 min. The formed precipitate was again dissolved by the addition of 1 mL $H_2O$. Di-*tert*-butyl dicarbonate (1.5 equiv., 10.6 mmol, 2.3 g) was dissolved in 5 mL anhydrous MeOH and slowly added to the reaction mixture, which was subsequently stirred at room temperatur for 4 h. After completion 10 mL $H_2O$ were added to the mixture and MeOH removed under reduced pressure. The obtained suspension was washed with $Et_2O$ twice, basified with 2 M NaOH solution and extracted with $CH_2Cl_2$. The combined organic phases were dried over $Na_2SO_4$ and the solvent removed under reduced pressure. The obtained crude product was dissolved in EtOAc and the solid residue removed over a patch of silica. The solvent was removed under reduced pressure to yield **13** as an off-white solid (1.38 g, 62%).

| | |
|---|---|
| **Melting Point** | 103-105 °C |
| **$^1$H NMR** (200 MHz, CDCl$_3$) | δ = 7.32 – 7.09 (m, 10H, *H*-arom), 5.81 (d, J = 8.51 Hz, 1H, C*H*-NH), 4.77 (brs, 1H, N*H*), 4.25 (d, J = 3.79 Hz, 1H, C*H*-NH$_2$), 1.38 (s, 2H, N*H*$_2$), 1.22 (s, 9H, C-(C*H*$_3$)$_3$). |
| **$^{13}$C NMR** (100 MHz, CDCl$_3$) | δ = 155.6 (s, NH-*C*O), 142.2 (s, *C*-arom), 141.0 (s, *C*-arom), 128.5 (d, *C*-arom), 128.3 (d, *C*-arom), 127.4 (d, *C*-arom), 127.2 (d, *C*-arom), 126.8 (d, *C*-arom), 126.4 (d, *C*-arom), 79.2 (s, *C*-(CH$_3$)$_3$), 60.0 (d, *C*H-NHCO), 59.9 (d, *C*H-NH$_2$), 28.3 (q, C-(*C*H$_3$)$_3$). |
| **HRMS** (ESI-TOF) | m/z: [M + H]$^+$ Calculated for C$_{19}$H$_{25}$N$_2$O$_2$ 313.1911; Found 313.1912 |
| **Specific Rotation** | α$_D$$^{20}$ = +34.4 (*c* 1.0, MeOH) |
| **ν$_{max}$/cm$^{-1}$** | 3378 (NH), 2977 (C–H ν), 1684 (C=O), 1514 (C=C), 1455 (C–H δ), 756 (C–H arom), 696 (C–H arom) |

### V.3.7 *N*-(((1*R*,2*R*)-1,2-diphenyl-2-(pyridine-3-ylmethyl)amino)ethyl)-carbamic acid, 1,1-dimethylethyl ester 14



**13**                                                                                                 **14**
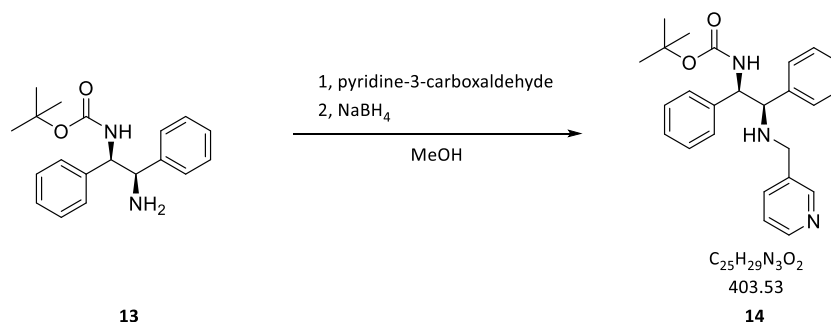
Compound **14** was prepared according to V.2.1 using **13** (1.0 equiv., 0.6 mmol, 200 mg), activated molecular sieve 4 Å (0.5 g) and freshly distilled pyridine-3-carboxaldehyde (1.0 equiv., 0.6 mmol, 60 μL) in 10 mL anhydrous MeOH. Subsequent reduction was performed with NaBH$_4$ (1.5 equiv., 0.9 mmol, 36 mg) at room temperature. The crude product was purified via silica column chromatography (15 g silica, PE:EtOAc 1:1 + Et$_3$N) to yield **14** as a colorless solid (166 mg, 64%).

| | |
|---|---|
| **Melting Point** | 90-91 °C |
| **$^1$H NMR** (400 MHz, CDCl$_3$) | δ = 8.39 (d, J = 4.05 Hz, 1H, *H*-pyridine), 8.28 (s, 1H, *H*-pyridine), 7.36 (d, J = 6.88 Hz, 1H, *H*-pyridine), 7.27 − 7.04 (m, 11H, *H*-pyridine, *H*-arom), 5.51 (d, J = 7.69 Hz, 1H, C*H*-NHCO), 4.78 (brs, 1H, N*H*-CO), 3.86 (s, 1H, C*H*-NH), 3.57 (d, J = 13.48 Hz, 1H, NH-C*H*$_2$), 3.34 (d, J = 13.48 Hz, 1H, NH-C*H*$_2$), 1.75 (brs, 1H, N*H*-CH$_2$), 1.27 (s, 9H, C-(C*H*$_3$)$_3$). |
| **$^{13}$C NMR** (100 MHz, CDCl$_3$) | δ = 155.5 (s, NH-*C*O), 149.5 (d, *C*-pyridine), 148.5 (d, *C*-pyridine), 140.2 (s, *C*-arom), 139.6 (s, *C*-arom), 135.6 (d, *C*-pyridine), 135.2 (s, *C*-pyridine), 128.4 (d, *C*-arom), 127.8 (d, *C*-arom), 127.6 (d, *C*-arom), 127.3 (d, *C*-arom), 126.5 (d, *C*-arom), 123.3 (d, *C*-pyridine), 79.5 (s, *C*-(CH$_3$)$_3$), 66.6 (d, *C*H-NH), 59.8 (d, *C*H-NHCO), 48.4 (t, NH-*C*H$_2$), 28.3 (q, C-(*C*H$_3$)$_3$). |
| **HRMS** (ESI-TOF) | m/z: [M + H]$^+$ Calculated for C$_{25}$H$_{30}$N$_3$O$_2$ 404.2333; Found 404.2333 |
| **Specific Rotation** | α$_D^{20}$ = +2.2 (*c* 1.25, MeOH) |
| **ν$_{max}$/cm$^{-1}$** | 3378 (N−H), 2976 (C−H ν), 1683 (C=O), 1510 (C=C), 1463 (C−H δ), 756 (C−H arom), 698 (C−H arom) |

### V.3.8    1-Butyl-3-((((1*R*,2*R*)-2-((*tert*-butoxycarbonyl)amino)-1,2-diphenylethyl)amino) methyl)pyridin-1-ium bromide 15



| | |
|---|---|
| **14** | **15** |
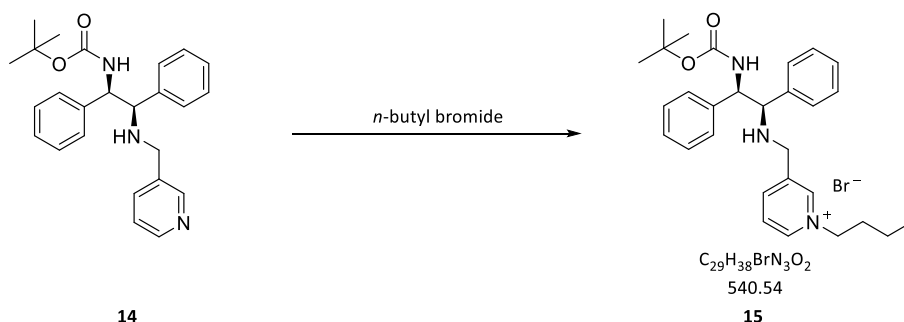
Finely powdered **14** (1.0 equiv., 1.8 mmol, 753 mg) was mixed with *n*-butyl bromide (1.2 equiv., 2.2 mmol, 307 mg), sealed and heated to 80 °C for 20 h. Excess *n*-butyl bromide was removed under reduced pressure to yield **15** as a yellow foam (1.0 g, >99%), which was used without further purification.

**¹H NMR** (400 MHz, MeOD)   $\delta$ = 8.83 (d, J = 5.87 Hz, 1H, *H*-pyridine), 8.78 (s, 1H, *H*-pyridine), 8.31 (d, J = 7.94 Hz, 1H, *H*-pyridine), 7.90 (t, J = 6.91 Hz, 1H, *H*-pyridine), 7.27 − 7.10 (m, 10H, *H*-arom), 4.55 (t, J = 7.25 Hz, 2H, N-C*H*₂), 4.03 (d, J = 7.94 Hz, 1H, C*H*-NH), 3.94 − 3.80 (m, 2H, NH-C*H*₂), 2.01 − 1.89 (m, 2H, N-CH₂-C*H*₂), 1.53 − 1.21 (m, 11H, N-(CH₂)₂-C*H*₂, C-(C*H*₃)₃ ), 1.02 (t, J = 7.25 Hz, 3H, N-(CH₂)₃-C*H*₃).

**¹³C NMR** (100 MHz, MeOD)   $\delta$ = 156.5 (s, NH-*C*O), 144.6 (d, *C*-pyridine), 143.5 (d, *C*-pyridine), 142.9 (s, *C*-arom), 142.4 (d, *C*-pyridine), 140.8 (s, *C*-pyridine), 139.9 (s, *C*-arom), 128.1 (d, *C*-arom), 128.0 (d, *C*-arom), 127.7 (d, *C*-arom), 127.2 (d, *C*-arom), 127.1 (d, *C*-arom), 126.7 (d, *C*-pyridine), 79.0 (s, *C*-(CH₃)₃), 67.2 (d, *C*H-NH), 61.3 (t, N-*C*H₂), 60.6 (d, *C*H-NHCO), 47.4 (t, NH-*C*H₂), 33.0 (t, N-CH₂-*C*H₂), 27.5 (q, C-(*C*H₃)₃), 19.1 (t, N-(CH₂)₂-*C*H₂), 12.6 (q, N-(CH₂)₃-*C*H₃).

**HRMS** (ESI-TOF)   m/z: [M]⁺ Calculated for C₂₉H₃₈N₃O₂ 460.2959; Found 460.2974

**Specific Rotation**   $\alpha_D{}^{20}$ = +20.1 (*c* 1.0, MeOH)

**v_max/cm⁻¹**   3245 (N−H), 2965 (C−H ν), 1691 (C=O), 1498 (C=C), 1463 (C−H δ), 756 (C−H arom), 699 (C−H arom)

### V.3.9    1-Butyl-3-((((1R,2R)-2-Amino-1,2-diphenylethyl)amino)methyl)pyridin-1-ium bromide 16



**15**    **16**
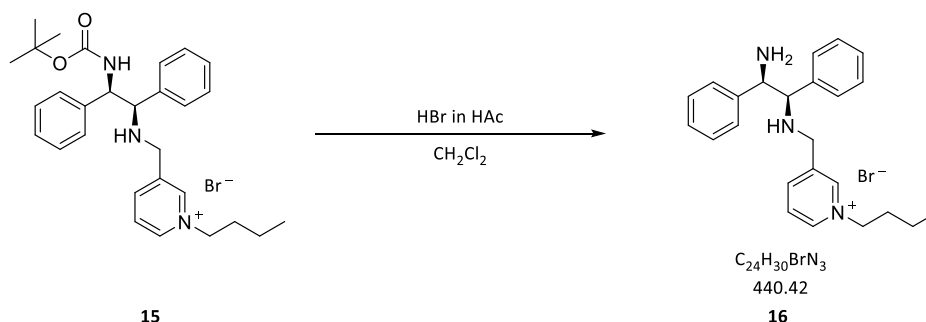
Reaction protocol adapted from literature.[50]

Compound **15** (1.0 equiv., 1.0 mmol, 540 mg) was dissolved in 20 mL $CH_2Cl_2$ and cooled via ice bath. Hydrogen bromide (33% in AcOH, 10 equiv., 10 mmol, 1.75 mL) was slowly added under Ar atmosphere. The reaction mixture was allowed to warm to room temperature and stirred for 4 h. After neutralization with saturated $Na_2CO_3$ solution the phases were separated and the aqueous phase extracted with $CH_2Cl_2$. The combined organic phases were dried over $Na_2SO_4$ and the solvent removed under reduced pressure. The crude product was purified via column chromatography (60 g silica, $MeOH/H_2O/AcOH$ 5:4:1), to yield **16** as orange foam (148 mg, 33%).

| | |
|---|---|
| **$^1$H NMR** (400 MHz, MeOD) | δ = 8.93 (s, 1H, *H*-pyridine), 8.83 (d, J = 6.20 Hz, 1H, *H*-pyridine), 8.46 (d, J = 7.97 Hz, 1H, *H*-pyridine),8.00 − 7.94 (m, 1H, *H*-pyridine), 7.18 − 7.09 (m, 10H, *H*-arom), 4.60 (t, J = 7.63 Hz, 2H, N-C*H₂*), 4.11 (d, J = 8.84 Hz, 1H, C*H*-NH₂), 3.91 (d, J = 15.46 Hz, 1H, NH-C*H₂*), 3.84 (d, J = 15.46 Hz, 1H, N*H*-CH₂), 3.80 (d, J = 8.84 Hz, 1H, C*H*-NH), 2.03 − 1.95 (m, 2H, N-CH₂-C*H₂*), 1.48 − 1.39 (m, 2H, N-(CH₂)₂-C*H₂*), 1.04 (t, J = 7.43 Hz, 3H, N-(CH₂)₃-C*H₃*). |
| **$^{13}$C NMR** (100 MHz, MeOD) | δ = 146.1 (d, *C*-pyridine), 145.4 (d, *C*-pyridine), 143.9 (d, *C*-pyridine), 143.7 (s, *C*-arom), 139.6 (s, *C*-arom), 136.0 (s, *C*-pyridine), 130.0 (d, *C*-arom), 129.8 (d, *C*-arom), 129.6 (d, *C*-arom), 129.3 (d, *C*-arom), 129.0 (d, *C*-arom), 128.6 (d, *C*-pyridine), 67.5 (d, *C*H-NH), 62.8 (t, N-*C*H₂), 61.4 (d, *C*H-NH₂), 48.8 (t, NH-*C*H₂), 34.5 (t, N-CH₂-*C*H₂), 20.5 (t, N-(CH₂)₂-*C*H₂), 13.8 (q, N-(CH₂)₃-*C*H₃). |
| **HRMS** (ESI-TOF) | m/z: [M]⁺ Calculated for $C_{24}H_{30}N_3$ 360.2434; Found 360.2435 |
| **Specific Rotation** | $\alpha_D{}^{20}$ = +76.8 (*c* 0.95, MeOH) |
| **$v_{max}$/cm⁻¹** | 3386 (N−H), 2944 (C−H ν), 1498 (C=C), 1453 (C−H δ), 698 (C−H arom) |

### V.3.10 1-Dodecyl-3-((((1R,2R)-2-((tert-butoxycarbonyl)amino)-1,2-diphenylethyl) amino)methyl)pyridin-1-ium bromide 17
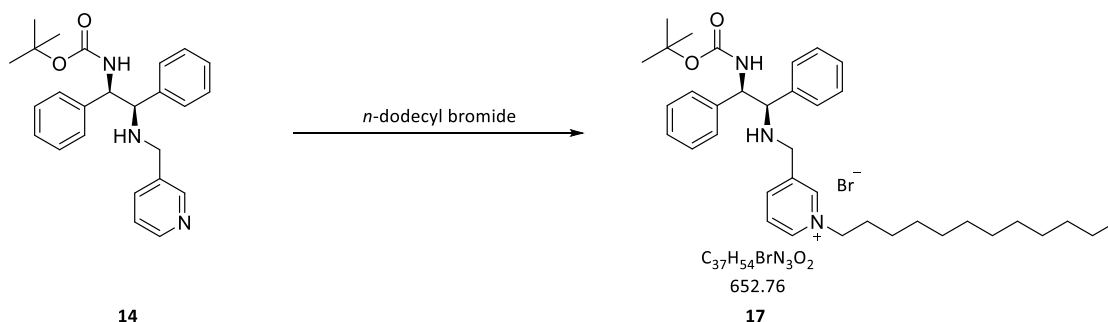


Finely powdered **14** (1.0 equiv., 1.2 mmol, 500 mg) was mixed with *n*-dodecyl bromide (1.2 equiv., 1.4 mmol, 370 mg), sealed and heated to 80 °C for 20 h. Excess *n*-dodecyl bromide was removed by refluxing the crude product with *n*-hexane. Remaining volatile compounds were removed under reduced pressure to yield **17** as an orange foam (800 mg, 99%). The product was used without further purification.

**¹H NMR** (400 MHz, MeOD)  $\delta$ = 8.86 − 8.80 (m, 2H, *H*-pyridine), 8.36 (d, J = 7.56 Hz, 1H, *H*-pyridine), 7.92 (t, J = 7.07 Hz, 1H, *H*-pyridine), 7.27 − 7.12 (m, 10H, *H*-arom), 4.88 (brs, 1H, C*H*-NHCO), 4.56 (t, J = 7.47 Hz, 2H, N-C*H₂*), 4.14 (brs, 1H, C*H*-NH), 4.01 − 3.87 (m, 2H, NH-C*H₂*), 2.03 − 1.93 (m, 2H, N-CH₂-C*H₂*), 1.47 − 1.25 (m, 27H, C-(C*H₃*)₃, N-(CH₂)₂-(C*H₂*)₉), 0.91 (t, J = 6.80 Hz, 3H, N-(CH₂)₁₁-C*H₃*).

**¹³C NMR** (100 MHz, MeOD)  $\delta$ = 157.8 (s, NH-*C*O), 146.2 (d, *C*-pyridine), 145.2 (d, *C*-pyridine), 144.0 (d, *C*-pyridine), 141.7 (s, *C*-arom), 137.9 (s, *C*-arom), 129.6 (d, *C*-arom), 129.4 (d, *C*-arom), 129.0 (d, *C*-arom), 128.9 (d, *C*-arom), 128.6 (d, *C*-arom), 128.4 (d, *C*-arom), 128.1 (d, *C*-pyridine), 80.5 (s, *C*-(CH₃)₃), 68.4 (d, *C*H-NH), 62.9 (t, N-*C*H₂), 61.6 (d, *C*H-NHCO), 33.0 (t, N-CH₂-*C*H₂), 32.4 (t, N-(CH₂)₂-*C*H₂), 30.6 (t, N-(CH₂)₃-*C*H₂), 30.6 (t, N-(CH₂)₄-*C*H₂), 30.4 (t, N-(CH₂)₅-*C*H₂), 30.4 (t, N-(CH₂)₆-*C*H₂), 30.1 (t, N-(CH₂)₇-*C*H₂), 28.7 (q, *C*-(CH₃)₃), 27.1 (t, N-(CH₂)₈-*C*H₂), 23.6 (t, N-(CH₂)₉-*C*H₂), 14.4 (q, N-(CH₂)₁₁-*C*H₃).

**HRMS** (ESI-TOF)  m/z: [M]⁺ Calculated for C₃₇H₅₄N₃O₂ 572.4211; Found 572.4215

**Specific Rotation**  $\alpha_D{}^{20}$ = +13.4 (*c* 1.05, MeOH)

**ν_max/cm⁻¹**  3248 (N−H), 2924 (C−H ν_a), 2853 (C−H ν_s), 1697 (C=O), 1495 (C=C), 1454 (C−H δ), 757 (C−H arom), 699 (C−H arom)

## V.4 General Procedure for the Enantioselective Transfer Hydrogenation of Aromatic Ketones with Chiral Ionic Ligands
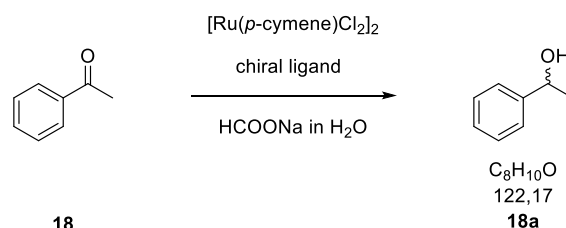


A 20 mg/mL stock solution of catalyst precursor [Ru($p$-cymene)Cl$_2$]$_2$ in HPLC-grade acetonitrile was freshly prepared. The stock solution (0.01 mmol, 6.12 mg, 306 µL) was transferred to a flame-dried Schlenk flask and the solvent was evaporated under reduced pressure for 2 h. The chiral ligand (2.1 equiv., 0.021 mmol) was dissolved in 4 mL water to result in a 5 mM solution. Water was purged with argon for 30 min prior to use. The solution of chiral ligand was added to the catalyst precursor in the Schlenk flask under argon atmosphere and stirred at 40 °C for 30 min to form the active catalyst. Subsequently, sodium formate (5.0 equiv., 10 mmol, 680 mg) was added and the mixture stirred until it was clear again. Then ketone **18** (2 mmol) was added and the reaction mixture stirred at 25 °C for 24 h. The reaction mixture was extracted with Et$_2$O, dried over Na$_2$SO$_4$ and the solvent removed under reduced pressure. The crude product was purified via column chromatography (PE/EtOAc) and the product alcohol **18a** analyzed via $^1$H NMR and chiral HPLC.

| | |
|---|---|
| **$^1$H NMR** (200 MHz, CDCl$_3$) | δ = 7.34 – 7.13 (m, 5H), 4.81 (q, J = 6.42 Hz, 1H), 1.82 (s, 1H), 1.42 (d, J = 6.45 Hz, 3H). |
| **Enantiomeric Excess** | 84% ee (*R*) |
| | Method (A); t$_r$(*R*) = 13 min, t$_r$(*S*) = 15 min |

Analytical data was in accordance with literature.[51]

## V.4.1　　　Kinetic Experiment

For the kinetic experiments the reaction mixture was prepared according to the general procedure in V.4. The experiments were conducted in a flame-dried Schlenk tube at 40 °C. After formation of the catalyst complex and addition of sodium formate, the reaction mixture was stirred for 10 min to collect background infrared spectra. Then acetophenone (2 mmol) was added and the reaction progress monitored via online infrared measurements, whereby reaction spectra were collected every minute. When no further conversion could be observed, the reactions were stopped and the reaction mixtures analyzed via HPLC to determine substrate conversion as a reference value.

## V.4.1　　　Kinetic Experiment

### V.4.2 Substate Scope

A variety of aromatic ketones were reduced according to procedure V.4. The obtained alcohols were analyzed via ^{1}H NMR and chiral HPLC. Analytical data was in accordance with the literature.[51–54]

#### V.4.2.1 *1-Phenylpropan-1-ol*



**19a**
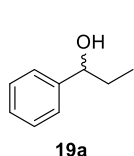
| | |
|---|---|
| **^{1}H NMR** (200 MHz, CDCl₃) | δ = 7.24 – 7.07 (m, 5H), 4.37 (t, J = 6.67 Hz, 1H), 2.61 (brs, 1H), 1.75 – 1.46 (m, 2H), 0.76 (t, J = 7.41 Hz, 3H). |
| **Enantiomeric Excess** | 84%ee (*R*) |
| | Method (A); $t_r$(*R*) = 11 min, $t_r$(*S*) = 12 min |

#### V.4.2.2 *1-(4-Chlorphenyl)ethanol*



**20a**
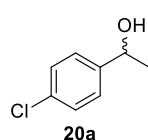
| | |
|---|---|
| **^{1}H NMR** (200 MHz, CDCl₃) | δ = 7.26 – 7.15 (m, 4H), 4.76 (t, J = 6.44 Hz, 1H), 2.13 (brs, 1H), 1.36 (d, J = 6.40 Hz, 3H). |
| **Enantiomeric Excess** | 84%ee (*R*) |
| | Method (A); $t_r$(*R*) = 14.9 min, $t_r$(*S*) = 14.3 min |

#### V.4.2.3 *1-(4-Methylphenyl)ethanol*



**21a**
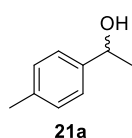
| | |
|---|---|
| **^{1}H NMR** (200 MHz, CDCl₃) | δ = 7.24 – 7.15 (m, 2H), 7.12 – 7.04 (m, 2H), 4.79 (q, J = 6.39 Hz, 1H), 2.27 (s, 3H), 1.73 (brs, 1H), 1.41 (d, J = 6.42 Hz, 3H). |
| **Enantiomeric Excess** | 97%ee (*R*) |
| | Method (C); $t_r$(*R*) = 18 min, $t_r$(*S*) = 16 min |

#### V.4.2.4 *1-(4-Methoxyphenyl)ethanol*



**22a**
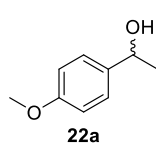
| | |
|---|---|
| **^{1}H NMR** (200 MHz, CDCl₃) | δ = 7.26 – 7.17 (m, 2H), 6.85 – 6.75 (m, 2H), 4.78 (q, J = 6.54 Hz, 1H), 3.72 (s, 3H), 1.73 (brs, 1H), 1.40 (t, J = 6.63 Hz, 3H). |
| **Enantiomeric Excess** | 42%ee (*R*) |
| | Method (A); $t_r$(*R*) = 21 min, $t_r$(*S*) = 22 min |

#### V.4.2.5 *1-(1-Naphtyl)ethanol*



**23a**
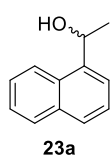
| | |
|---|---|
| **^{1}H NMR** (200 MHz, CDCl₃) | δ = 8.14 – 7.41 (m, 7H), 5.56 (q, J = 6.44 Hz, 1H), 3.35 (brs, 1H), 1.66 (d, J = 6.71 Hz, 3H) |
| **Enantiomeric Excess** | 93%ee (*R*) |
| | Method (B); $t_r$(*R*) = 12 min, $t_r$(*S*) = 9 min |

# VI  Appendix

## VI.1  List of Abbreviations

| | | | |
|---|---|---|---|
| A$^-$ | anion | HRMS | high resolution mass spectrometry |
| AcOH | acetic acid | CIL | chiral ionic ligand |
| Ar | argon | *i*-PrOH | *iso*-propanol |
| BINOL | [1,1'-binaphthalene]-2,2'-diol | MeOH | methanol |
| BOC | tert-butyloxycarbonyl | MPLC | medium pressure liquid chromatography |
| CH$_2$Cl$_2$ | Dichloromethane | | |
| CH$_2$O | Formaldehyde | NaOH | sodium hydroxide |
| CIL | chiral ionic ligand | Na$_2$SO$_4$ | sodium sulfate |
| ee | enantiomeric excess | NEt$_3$ | Triethylamine |
| EtOAc | ethyl acetate | PE | petrol ether |
| Et$_2$O | diethyl ether | o.n. | over night |
| EtOH | ethanol | *p*-TsOH | *p*-toluene sulfonic acid |
| equiv. | molar equivalent | rt | room temperature, 25 °C |
| H$_2$N-NH$_2$ | hydrazine | TFA | trifluoro acetic acid |
| HCl | hydrochloric acid | TLC | thin layer chromatography |
| HCO$_2$H | formic acid | TMS | trimethylsilyl |
| HCO$_2$Na | sodium formate | | |
| HPLC | high pressure liquid chromatography | | |

## VI.2  References

(1)     Anastas, P. T.; Warner, J. C. *Green chemistry : theory and practice*; Oxford University Press, 1998.

(2)     Sabatier, P. Paul Sabatier - Nobel Lecture: The Method of Direct Hydrogenation by Catalysis https://www.nobelprize.org/nobel_prizes/chemistry/laureates/1912/sabatier-lecture.html (accessed Jan 16, 2017).

(3)     Sheldon, R.; Arends, I.; Hanefeld, U. *Industrial Catalysis: A practical approach, Second Edition*; Wiley-VCH Verlag GmbH & Co. KGaA: Weinheim, Germany, 2006.

(4)     Rylander, P. N. In *Ullmann's Encyclopedia of Industrial Chemistry*; Wiley-VCH Verlag GmbH & Co. KGaA: Weinheim, Germany, 2000.

(5)     Noyori, R.; Hashiguchi, S. *Acc. Chem. Res.* **1997**, *30*, 97–102.

(6)     Palmer, M.; Wills, M. *Tetrahedron: Asymmetry* **1999**, *10*, 2045–2061.

(7)     Ikariya, T.; Blacker, A. J. *Acc. Chem. Res.* **2007**, *40*, 1300–1308.

(8)     Osborn, J. A.; Jardine, F. H.; Young, J. F.; Wilkinson, G. *J. Chem. Soc. A* **1966**, 1711.

(9)     Dub, P. A.; Gordon, J. C. *Dalton Trans.* **2016**, *45*, 6756–6781.

(10)    Zassinovich, G.; Mestroni, G.; Gladiali, S. *Chem. Rev.* **1992**, *92*, 1051–1069.

(11)    Meerwein, H.; Schmidt, R. *Justus Liebigs Ann. Chem.* **1925**, *444*, 221–238.

(12)    Ponndorf, W. *Angew. Chem.* **1926**, *39*, 138–143.

(13)    Verley, A. *Bull. Soc. Chim. Fr.* **1925**, *37*, 537–542.

(14)    Trocha-Grimshaw, J.; Henbest, H. B. *Chem. Commun.* **1967**, *11*, 544–544.

(15)    Sasson, Y.; Blum, J. *Tetrahedron Lett.* **1971**, *12*, 2167–2170.

(16)    Bäckvall, J.-E. *J. Organomet. Chem.* **2002**, *652*, 105–111.

(17)    Gladiali, S.; Alberico, E. *Chem. Soc. Rev.* **2006**, *35*, 226–236.

(18)    Wu, X.; Xiao, J. *Chem. Commun.* **2007**, 2449–2466.

(19)    Corey, E. J.; Bakshi, R. K.; Shibata, S. *J. Am. Chem. Soc.* **1987**, *109*, 5551–5553.

(20)    Noyori, R.; Tomino, I.; Tanimoto, Y.; Nishizawa, M. *J. Am. Chem. Soc.* **1984**, *106*, 6709–6716.

(21)    Ohkuma, T.; Ooka, H.; Hashiguchi, S.; Ikariya, T.; Noyori, R. *J. Am. Chem. Soc.* **1995**, *117*, 2675–2676.

(22)    Noyori, R.; Ohkuma, T. *Angew. Chem. Int. Ed.* **2001**, *40*, 40–73.

(23)    Wang, D.; Astruc, D. *Chem. Rev.* **2015**, *115*, 6621–6686.

(24)    Hashiguchi, S.; Fujii, A.; Takehara, J.; Ikariya, T.; Noyori, R. *J. Am. Chem. Soc.* **1995**, *117*, 7562–7563.

(25)    Haack, K.-J.; Hashiguchi, S.; Fujii, A.; Inoue, S.; Ikariya, T.; Noyori, R. *Angew. Chem. Int. Ed.* **1997**, *36*, 285–288.

(26)    Koike, T.; Ikariya, T. *Adv. Synth. Catal.* **2004**, *346*, 37–41.

(27)    Noyori, R.; Yamakawa, M.; Hashiguchi, S. *J. Org. Chem.* **2001**, *66*, 7931–7944.

(28)    Clapham, S. E.; Hadzovic, A.; Morris, R. H. *Coord. Chem. Rev.* **2004**, *248*, 2201–2237.

(29)    Wu, X.; Li, X.; Hems, W.; King, F.; Xiao, J. *Org. Biomol. Chem.* **2004**, *2*, 1818.

(30)    Handgraaf, J. W.; Meijer, E. J. *J. Am. Chem. Soc.* **2007**, *129*, 3099–3103.

(31)    Dub, P. A.; Ikariya, T. *J. Am. Chem. Soc.* **2013**, *135*, 2604–2619.

(32)    Zhu, M. *Catal. Lett.* **2016**, *146*, 575–579.

(33)    Hayes, A.; Clarkson, G.; Wills, M. *Tetrahedron: Asymmetry* **2004**, *15*, 2079–2084.

(34)    Zhou, S.; Fleischer, S.; Junge, K.; Das, S.; Addis, D.; Beller, M. *Angew. Chem. Int. Ed.* **2010**, *49*, 8121–8125.

(35)    Foubelo, F.; Yus, M. *Chem. Rec.* **2015**, *15*, 907–924.

(36)    Martins, J. E. D.; Clarkson, G. J.; Wills, M. *Org. Lett.* **2009**, *11*, 847–850.

(37)    Sheldon, R. A. *Green Chem.* **2005**, *7*, 267–278.

(38)    Wu, X.; Liu, J.; Di Tommaso, D.; Iggo, J. A.; Catlow, C. R. A.; Bacsa, J.; Xiao, J. *Chem. Eur. J.* **2008**, *14*, 7699–7715.

(39)    Wu, X.; Li, X.; King, F.; Xiao, J. *Angew. Chem. Int. Ed.* **2005**, *44*, 3407–3411.

(40)    Ogo, S.; Abura, T.; Watanabe, Y. *Organometallics* **2002**, *21*, 2964–2969.

(41)    Ma, Y.; Liu, H.; Chen, L.; Cui, X.; Zhu, J.; Deng, J. *Org. Lett.* **2003**, *5*, 2103–2106.

(42)    Li, J.; Tang, Y.; Wang, Q.; Li, X.; Cun, L.; Zhang, X.; Zhu, J.; Li, L.; Deng, J. *J. Am. Chem. Soc.* **2012**, *134*, 18522–18525.

(43)    Vasiloiu, M.; Gaertner, P.; Zirbs, R.; Bica, K. *Eur. J. Org. Chem.* **2015**, 2374–2381.

(44)    Lee, D. W.; Ha, H.; Lee, W. K. *Synth. Commun.* **2007**, *37*, 737–742.

(45)    Demmans, K. Z.; Ko, O. W. K.; Morris, R. H. *RSC Adv.* **2016**, *6*, 88580–88587.

(46)    Guduguntla, S.; Hornillos, V.; Tessier, R.; Fañanás-Mastral, M.; Feringa, B. L. *Org. Lett.* **2016**, *18*, 252–255.

(47)    Vasiloiu, M.; Leder, S.; Gaertner, P.; Mereiter, K.; Bica, K. *Org. Biomol. Chem.* **2013**, *11*, 8092–8102.

(48)    Huang, H.; Zong, H.; Shen, B.; Yue, H.; Bian, G.; Song, L. *Tetrahedron* **2014**, *70*, 1289–1297.

(49)    da Silva, R. A.; Estevam, I. H. S.; Bieber, L. W. *Tetrahedron Lett.* **2007**, *48*, 7680–7682.

(50)    Tiffner, M.; Novacek, J.; Busillo, A.; Gratzer, K.; Massa, A.; Waser, M. *RSC Adv.* **2015**, *5*, 78941–78949.

(51)    Swizdor, A.; Janeczko, T.; Dmochowska-Gladysz, J. *J. Ind. Microbiol. Biotechnol.* **2010**, *37*, 1121–1130.

(52)    Ito, J.; Teshima, T.; Nishiyama, H. *Chem. Commun.* **2012**, *48*, 1105–1107.

(53)    Hayes, A. M.; Morris, D. J.; Clarkson, G. J.; Wills, M. *J. Am. Chem. Soc.* **2005**, *127*, 7318–7319.

(54)    Kagohara, E.; Pellizari, V. H.; Comasseto, J. V.; Andrade, L. H.; Porto, A. L. M. *Food Technol. Biotechnol.* **2008**, *46*, 381–387.